UNIVERSITY OF NAIROBI

SCHOOL OF PHYSICAL SCIENCES

DEPARTMENT OF CHEMISTRY

PREDICTION OF WOOD DENSITY AND CARBON-NITROGEN CONTENT IN TROPICAL AGROFORESTRY TREE SPECIES IN WESTERN KENYA USING INFRARED SPECTROSCOPY

BY

OLALE OWUOR KENNEDY

I56/79094/2009

A THESIS SUBMITTED IN PARTIAL FULFILLMENT FOR THE DEGREE OF MASTER OF SCIENCE IN CHEMISTRY OF THE UNIVERSITY OF NAIROBI

2012

DECLARATION

This research thesis is my original work and has not been presented for a degree in any other university.

Kennedy Owuor Olale

Reg no.I56/79094/2009

Signature..Date....16·11·2012

SUPERVISORS

Prof. Abiy Yenesew

Department of Chemistry

University of Nairobi

P.O Box 30197, Nairobi

Signature..Date.......16/11/2012

Dr. Keith Shepherd

World Agroforestry Centre (ICRAF)

P.O. Box 30677, Nairobi

Signature..Date....16·11·2012

Dr. Ramni Jamnadass

World Agroforestry Centre (ICRAF)

P.O. Box 30677, Nairobi

Signature..Date.......16ᵃ Nov 2012.

DEDICATION

To my late Father Mr. Alloys Olale who made it possible for me to go to school.

ACKNOWLEDGMENT

TABLE OF CONTENTS

LIST OF TABLES

LIST OF FIGURES

ACRONYMES

FTIR	Fourier Transform Infrared
GEF	Global Environmental Fund
GWD	Global Wood density Database
IR	Infrared Spectroscopy
MIR	Mid Infrared Spectroscopy
MLR	Multiple Linear Regressions
MSC	Multiplicative Scatter Correction
NIR	Near Infrared Spectroscopy
PCA	Principle Component Analysis
PCs	Principle Components
PLS	Partial Least Squares
PLSR	Partial Least Squares Regression
RMSEP	Root Mean Square Error of Prediction
RPD	Ratio performance deviation
SEC	Standard Error of Calibration
SECV	Standard Error of Cross Validation
SEP	Standard Error of Prediction
SNV	Standard Normal Variate
SSR	Sum Squares of Regression
TSS	Total Sum of Squares
UNEP	United Nations Environmental Program
WKIEMP	Western Kenyan Integrated Management Project

ABSTRACT

The global debate on climate change needs to be furnished with accurate and precise measurement of biomass in agricultural landscapes. Wood density is a supporting parameter for biomass estimation; however, empirical methods for wood density determination are destructive and complex, as are conventional wet chemistry analyses of carbon and nitrogen. Thus a low cost and non-destructive method of estimation is required. Infrared Spectroscopy coupled with chemometrics multivariate techniques offers a fast and non-destructive alternative for obtaining reliable results without complex sample pre-treatments. This study sought to develop a prediction model for estimation of wood density, carbon and nitrogen across species using Infrared Spectroscopy.

Empirical data for determination of these parameters were obtained from coring 77 trees sampled from three benchmark sites (Lower, Middle and Upper Yala blocks) along Yala basin in Western Kenya. Samples from cored holes in the tree (branch, stem and roots) were used to estimate wood biovolume and density. Models for estimation of these parameters were derived from scanning 404 cores using diffuse reflectance Infrared Spectroscopy and reference values for carbon and nitrogen obtained using a Carbon-Nitrogen analyzer. Partial least squares regression, using first derivative spectra pre-treatment, was used to develop a model based on different calibrations sets. Models were compared on the basis of the accuracy of prediction using the coefficient of determination (R^2), Standard Error of Calibration (SEC) and Standard Error of Prediction (SEP).

Calculated wood density range was 0.20-0.95gcm^{-3} with the mean being 0.59 gcm^{-3}, while IR predicted 0.25-0.95 gcm^{-3} (mean 0.53 gcm^{-3}) in the Near Infrared Region (NIR) and 0.32-0.86 gcm^{-3} (mean 0.53 gcm^{-3}) in the Mid Infrared Region (MIR). Measured carbon range was 40%-52% (mean 48%), while IR predicted 44%-51% (mean 48%) in NIR region and 46%-51% (mean 48%) in MIR region. Measured nitrogen range was 0.09-0.48% (mean 0.28%), while IR predicted 0.18%-0.47% (mean 0.24%) in NIR region and 0.18%-0.38% (mean 0.24%) in MIR region. Values of SEC were low relative to laboratory analytical errors. Interactions between densities with tree species and tree parts showed significant effect (p<0.001), while the interactions between tree parts and species showed no significant effect. Values averaged to the species level predicted much better than the individual core models with R^2>0.57 for all the parameters. This suggests large variations within species that cannot be predicted using IR.

The data generated here on densities were comparable with those given in a global wood density database. On the other hand, carbon content varied among species but not between the sites, an indication that the often assumed default value of 50% carbon in wood is over estimation of tree carbon and would lead to over estimation of the total carbon stocks. NIR region gave better predictions than MIR, although the prediction performance was insufficient to recommend Infrared Spectroscopy as a practical method for direct determination of wood density and carbon content across species when different percentages were used.

CHAPTER ONE

INTRODUCTION

1.1 General

Landscape monitoring approaches that deals with complex tropical agroforestry systems can provide opportunities for smallholders to benefit from carbon trading (Shepherd and Walsh, 2007). Rapid measurements of tree biovolume has been done from field surveys but information on density (specific gravity) and carbon content of tropical tree species is sparse. Research to acquire this information by developing rapid and low cost method and a model that can be applied across species is needed. In addition, there is need for a better understanding in assessing the variation in wood density and carbon concentrations among different species as density is related to wood quality traits (Pliura *et al.*, 2007).

Infrared (IR) Reflectance Spectroscopy is a promising tool for rapid assessment of physical and chemical parameters such as density, carbon and nitrogen contents for trees (Shepherd and Walsh, 2007). The spectroscopic technique utilizes the specificity of absorption frequencies of the molecules owing to the fact that molecules rotate or vibrate by absorbing discrete energies (Hoffmeyer and Pedersen, 1995). The frequencies of these vibrations are determined by the shape of the molecular potential energy surfaces, the masses of the atoms, the bond strength and associated vibronic coupling (Sherman, 1997).

This method has been extended to assess non-chemical characteristics of solid wood and showed capability for determination of mechanical, anatomical and physical properties, including basic densities (Hein and Chaix, 2009), determination of constituents in dried and ground wood (Mroczyk*et al.,* 1992; Hoffmeyer and Pedersen, 1995), and moisture content (Pedersen *et al.,* 1993).

The technique is non-destructive for evaluation of organic materials where particularly C–H, O–H, and N–H groups influence the properties to be assessed (Hoffmeyer and Pedersen, 1995). The technique is based on the principle of Lamberts-Beer law and its ability to measure C–H, O–H, and N–H bonds and extends its application to all biological materials including plant materials (Shepherd and Walsh, 2007).

IR Spectroscopy has been applied to both developed and developing countries particularly in agriculture for soil carbon and plant analysis but with limited use in poorer developing countries (Shepherd and Walsh, 2007). However, the high potential of IR Spectroscopy in accelerating agricultural development, at the same time safe-guarding the environment in these poorer countries in achieving millennium development goals has been recognised (Shepherd and Walsh, 2007).

Apart from the potential contribution of agricultural landscapes as carbon sinks, forests are the greatest essential source of oxygen in the world and acts as carbon dioxide store (Lindzen, 1997). Carbon dioxide, among other greenhouse gases is an influential gas leading to climate change (Lindzen, 1997). Therefore, estimation of carbon and wood density in trees across species using a single calibration model is necessary for assessment of above ground biomass in forest ecosystems.

2

Acquiring information on wood density is vital in gathering information on how much carbon is stored by a plant, as the density of wood depends on specific gravity and moisture content (Costa *et al.*, 2009). However, trees do vary in their phenotypic traits, resulting from both genetic responses to selection pressures and phenotypic responses to the environment (Costa *et al.*, 2009). Prediction of tree properties (physical and chemical) using IR Spectroscopy have not been extensively explored, unlike in soils where constituent soil properties have been predicted using both the Mid-Infrared and Near-Infrared region of the spectra (Ludwig *et al.*, 2008).

In a study by Ludwig *et al.* (2008) on soil constituent prediction using IR Spectroscopy, Mid-Infrared Spectroscopy (MIR) gave superior performance to Near-Infrared Spectroscopy (NIR). However, the use of MIR region is still not sufficiently explored in tree property assessment. The superiority of MIR method is based on the assumption that the Mid-IR region is dominated by intense fundamental vibrational bands, whereas the Near-IR region is dominated by much weaker and broader signals from vibration overtones and combination bands (Janik *et al.*, 1998; Ludwig *et al.*, 2008; McCarty *et al.*, 2002).

Studies in the diffuse-reflectance mode by Madari *et al.* (2006) and Ludwig *et al.* (2008) have challenged the assumed superiority and usefulness of MIR region in comparison with NIR in predicting soil constituents. Therefore, there is need to evaluate the usefulness of both MIR and NIR and analyze their spectra across tree species to derive a meaningful conclusion.

3

1.2 Problem Statement and Justification

The currently available method of estimating carbon stored in live trees involves cutting down the trees, taking sample discs from different parts and then drying these discs (Kirby and Potvin, 2007). The dry weight (biomass) is then converted to carbon content, this method is accurate for a particular location, but has major short comings: It is destructive, time consuming, expensive, and therefore impractical for large scale analysis. This study proposes a reliable method for estimation of the physical and chemical parameters of trees using Infrared Spectroscopy coupled with multivariate analysis techniques. The main benefit of this method is the replacement of the more expensive and time-consuming analytical methods with less destructive method involving tree coring using carpenters auger for samples collection.

The assessment of the contribution of agricultural landscapes to global carbon budgets depends on the accuracy in estimation of agricultural landscapes carbon. Currently an estimate of 50% carbon for woody tissues and 45% for foliage and fine roots is widely accepted as a constant factor for conversion of biomass to carbon stock (Houghton, 1996; Quanzhi *et al.*, 2009). This estimation using 50% default conversion factor for carbon introduces 10% bias in biomass estimation (Quanzhi *et al.*, 2009). The value is bound to change depending upon the tree species and biomass tissue sampled, thus the need for accuracy in carbon and density estimation to reduce the uncertainties in biomass carbon estimation.

1.3 Hypotheses

1. IR calibration models can be constructed to predict wood density and carbon concentration both within and across species in a single calibration.

2. There is variation in wood density and carbon concentration within and among species.

1.4 Objectives

The main objective was to develop Infrared prediction model for estimation of wood density, carbon and nitrogen concentrations across species in western Kenya landscapes.

Specific objectives are:

1. To develop a protocol for core sampling and infrared prediction of wood density and carbon concentration.

2. To develop a model for predicting wood density, carbon and nitrogen concentration for selected tree species in Western Kenya landscapes.

3. To establish the difference and/or similarities of MIR and NIR regions of spectra in the prediction of wood density, carbon and nitrogen concentrations across species.

CHAPTER TWO

LITERATURE REVIEW

2.1 Carbon sequestration in tropical forests

Tropical forests are considered as global source of biological diversity, carbon dioxide sink as well as source of livelihood, food and economic security for millions of people (Dewar, 1990). Clearance of tropical forests has resulted in increased amounts of carbon dioxide accumulation in the atmosphere, consequently leading to the interference with the role played by forests as carbon pools in the global carbon cycle (Dewar, 1990).

Carbon dioxide is usually taken up by forest ecosystems and stored as carbon in biomass (trunks, branches, foliage, and roots) and soils (Quanzhi *et al.,* 2009); these contribute to the reduction of greenhouse gas effect and stabilized climatic system (Quanzhi *et al.,* 2009). FAO (1999) estimated 13 million hectares of tropical forest loss each year to deforestation, emitting between 5.6 and 8.6 Giga tonnes of carbon dioxide (Houghton *et al.,* 1995).

Forests and forest soils may store as much as 2000 billion tonnes (Bt) of carbon (C), or 1500 Bt of carbon for soils alone (Gribbin, 1990). However, less attention has been laid to the carbon stored in various tropical agroforestry landscapes. Thompson and Matthews (1989) studied the amounts of carbon stored in different timber tree species by comparing carbon storage with tree different end uses, within the context of the United Kingdom. The model Matthews (1989) developed combined tree production curve with

estimates from the retention curves for carbon after felling. This kind of study however, was destructive resulting in deforestation. The development of less destructive method to estimate carbon content in timber is important for biodiversity preservation and may mitigate global climate change by reducing the release of carbon stored in trees and soils (Gribbin, 1990).

2.2 Climate change: the role of carbon and nitrogen

The global nitrogen (N) cycle is more severely altered by human activity than the global carbon (C) cycle, and reactive N dynamics affect all aspects of climate change considerations, including mitigation, adaptation, and impacts (Suddick *et al.*, 2012). Magnani *et al.* (2007) found that carbon (C) sequestration of temperate and boreal forests is clearly driven by nitrogen (N) deposition.

Nitrogen saturation implies a change in nitrogen cycling pattern from a closed internal cycle to an open cycle where excess nitrogen is leached and/or emitted from the forest ecosystem (Magnani *et al.*, 2007). The pattern of forest ecosystem and nitrogen circle can vary enormously depending on vegetation and previous activities at the site (Norby *et al.*, 2010). Carbon allocation in tree species is dependent on species composition and ecosystem age structure; the temperature changes and disturbances like forest fire affect the net carbon exchange (Juday *et al.*, 2010).

Tropical forest fire has been a challenge in carbon estimation in forests by affecting the carbon cycle in the following ways: It releases carbon to the atmosphere, converts relatively decomposable plant material into stable charcoal, re-initiates succession and

changes the ratio of forest-stand age classes and age distribution, alters the thermal and moisture regime of the mineral soil and remaining organic matter which strongly affects rates of decomposition and increases the availability of soil nutrients through conversion of plant biomass in to ash each at different timescales (Juday *et al.*, 2010).

2.3 Agricultural landscape mosaics: the case of western Kenya

In 2009, Carbon Benefits Project (CBP) - an initiative of United Nations Environment Programme (UNEP), the World Agroforestry Centre, along with a range of other key partners funded by the Global Environment Facility (GEF)-was launched to assess levels of carbon stored in trees *via* sustainable and climate-friendly land management. In this regard, Yala basin a catchments in and around Lake Victoria region was chosen as a test-bed for calculating how much carbon can be stored in trees when the land is managed in a sustainable and climate-friendly ways (UNEP, 2009).

This initiative is key to unlock the multi-billion dollar carbon market for millions of farmers, foresters and conservationists across developing world. The Yala basin, previously identified by the Western Kenyan Integrated Management Project (WKIEMP) covers an area of 3,351 km^2 (Boye *et al.*, 2008) consisting of three Blocks: Middle Yala, Upper Yala and Lower Yala with elevation ranges between 1200 and 1450 m.The three Block have vairied land use patterns as shown in Table 1 with the majority (75%) of the farmers practicing agroforestry.

Lower Yala block is located in Kisumu and Siaya counties and characterized by low to medium gradient hills, shallow depressions and small permanent streams (Boye *et al.*,

2008); the area is largely agricultural with some rangeland and thickets, few remnant forests are also present in Tiriki east area of the block.

Middle Yala block is located in Vihiga and Kakamega counties with Kaimosi forest found in this area. It is characterized by numerous small streams and wetlands of about 22% with elevation ranging from 1430 to 1720 m, common soil types are clay (46%) and silty clay soils (32%) (Boye *et al.,* 2008).

Upper Yala block is in Uasin Gishu county and generally characterized by level terrain at a relatively higher altitude between 2100 m to 2400 m above sea level (a.s.l). In general there are few trees in these landscapes.

Table 1: Primary land use among the three blocks of Yala.

Land use	Lower Yala	Middle Yala	Upper Yala
Food / beverage	43%	69%	48%
Forage	55%	28%	56%
Timber / fuel wood	12%	19%	8%
Other	4%	8%	3%

Source: Boye et al., (2008).

2.4 Wood chemistry

Wood is a porous material, consisting of a matrix of fibre walls and air spaces (voids within fibre walls); with fibre walls (solid-wood substance) considered to be constant for all wood species (Jozsa and Middleton, 1994). In relation, wood density provides a simple measure of the total amount of solid-wood substance in a piece of wood. For this reason, wood density provides an excellent means of predicting end-use characteristics of

9

wood such as strength, stiffness, hardness, heating value, machinability, pulp yield and paper making quality (Jozsa and Middleton, 1994).

Wood has two major chemical components: lignin (18–35%) and carbohydrate (65–75%) (Pettersen, 1984). There are other minor amounts of extraneous materials which occur in the form of organic extractives and inorganic minerals (ash) at a composition of about 4–10% (Pettersen, 1984). Table 2 shows elemental composition of wood according to Pettersen (1984).

Table 2: Average elemental composition of wood.

Elements	Share, % of dry matter weight
Carbon	45-50%
Hydrogen	6.0-6.5%
Oxygen	38-42%
Nitrogen	0.1-0.5%
Sulphur	Max 0.05

Source: Pettersen (1984).

The carbohydrate and lignin are the building blocks of a tree's cellular structure (Pettersen, 1984). Carbohydrate portion of wood comprises cellulose and the hemicelluloses, and these are primarily the composition of cell walls. The cell walls are held together by lignin giving the tree wood strength and rigidity.

2.4.1 Lignin

Lignin is a phenolic substance consisting of an irregular array of variously bonded hydroxy- and methoxy-substituted phenylpropane units responsible for the strength and rigidity of wood and binds together cellulose fibers (Pettersen, 1984). The precursor

molecules of lignin biosynthesis are hydroxy-cinnamylalcohols (monolignols) (Christophe and Grégoire, 2001): *p*-coumaryl alcohol, coniferyl alcohol, and sinapyl alcohol (Figure 1).

These alcohols are linked in lignin by carbon-oxygen and carbon–carbon bonds. However, the major difference among the precursor molecules of lignin biosynthesis is their degree of methoxylation (Christophe and Grégoire, 2001).
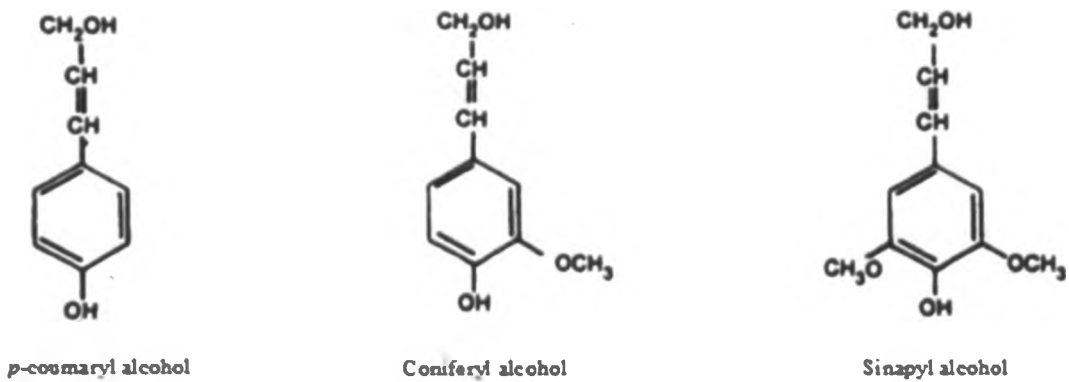
Figure 1: Precursors of lignin biosynthesis.

Lignin embeds the polysaccharide matrix giving rigidity and cohesiveness to the wood tissue (Christophe and Grégoire, 2001). Lignin being more hydrophilic provides hydrophilic surface needed for the transport of water, the lignin content and monomeric composition vary widely among different taxa, individuals, tissues, cell types, and cell wall layers (Christophe and Grégoire, 2001).

2.4.2 Carbohydrates

The carbohydrate portions of wood comprise cellulose and hemicelluloses. Between 40% and 50% of the dry wood weight consists of cellulose (Christophe and Grégoire, 2001)

and 25% to 35% hemicelluloses (Pettersen, 1984). The fundamental structural units are the microfibrils (MFs), which result through strong inter and intra molecular hydrogen bonds.

2.4.3 Cellulose

The microfibrils which are water-insoluble cellulose are associated with mixtures of soluble noncellulosic polysaccharides, the hemicelluloses. Cellulose occurs as heteropolymer such as glucomannan, galactoglucomannan, arabinogalactan, and glucuronoxylan, or as a homopolymer like galactan, arabinan, and 1,3-glucan (Christophe and Grégoire, 2001). Glucan polymer consists of linear chains of 1,4-bonded anhydroglucose units.

The number of sugar units in one molecular chain is referred to as the degree of polymerization (DP). Cellulose is insoluble in most solvents including strong alkali and becomes difficult to isolate from wood in pure form because of it's intimately association with the lignin and hemicelluloses (Pettersen, 1984). Cellulose consists of 6-carbon sugar units, glucose, while hemicellulose contains a mixture of 5 and 6-carbon sugars.

2.4.4 Hemicelluloses

Unlike cellulose, hemicelluloses are soluble in alkali and easily hydrolyzed by acids (Pettersen, 1984). They are synthesized in wood almost entirely from glucose, mannose, galactose, xylose, arabinose, 4-O- methyl-glucuronic acid, and galacturonic acid residues (Pettersen, 1984). Hemicelluloses are of much lower molecular weight than cellulose and

are present in abnormally large amounts when the plant is under stress; for example, compressed wood has higher lignin content (Pettersen, 1984). In hemicelluloses the C-6 sugars are the glucoses, galactoses and mannoses that make up galactoglucomannansin hardwoods. Xyloses and arabinose constitute the C-5 sugars in hemicelluloses.

2.4.5 Extraneous components

Extraneous components are extractives and ash in wood mostly soluble in neutral solvents (Pettersen, 1984). Extractives are a variety of organic compounds including fats, waxes, alkaloids, proteins, simple and complex phenolics, simple sugars, pectins, mucilages, gums, resins, terpenes, starches, glycosides, saponins, and essential oils (Pettersen, 1984); while ash is the inorganic residue remaining after ignition at high temperature (Pettersen, 1984). The extraneous components do not contribute to the cell wall structure and consist of 4– 10% of the dry weight of normal wood in temperate climates and as much as 20% of the dry weight of tropical species (Pettersen, 1984).

2.5 Infrared spectral region

Infrared Reflectance (IR) deals with the electromagnetic spectrum ranging from 700 to 10^6 nanometres (10 to 14300 cm^{-1}) as shown in table 3. The atoms in a chemical bond in this region continuously vibrate at discrete energy levels with respect to each other (Banwell, 1972).

IR works on the principle that when the target material is illuminated with Infrared light, IR energy is absorbed by functional groups made up of atoms and molecule; the

13

absorbed energy causes bending, stretching, and twisting of bonds which leads to the characteristic absorbance and reflectance patterns (Chalmers and Griffiths, 2002; Ichami, 2005).

The IR portion of the electromagnetic radiation (Table 3) is sub-divided into near infrared (NIR) 12500-4000 cm^{-1}, Mid Infrared (MIR) 4000-400 cm^{-1} and Far infrared 400 cm^{-1} (Osborne *et al.,* 1993). The NIR region (12500-4000 cm^{-1}) spectral features arise from combinations and overtones of the fundamental vibrations associated with C-H, O-H, and N-H bonds (Small, 2006) and is further divided into three sub-regions (combination, first overtone, and short wavelength) on the basis of spectral characteristics associated with each (Small, 2006).

Table 3: A summary of the Infrared region of the electromagnetic spectrum.

Region	Characteristic Transition	Wavelength range (nm)	Wave number range (cm^{-1})
Near-Infrared (NIR)	Overtones combination	700-2500	12500-4000
Middle-Infrared (MIR)	Fundamental Vibrations	$2500-5 \times 10^4$	4000-400
Far-Infrared	Rotations	$5 \times 10^4 - 10^6$	400-10

Source: Banwell (1972).

Typical principal characteristics of spectral bands found in the NIR region; first-overtone O-H stretch vibration near 6930 cm^{-1} and an O-H combination band near 5190 cm^{-1} also visible near 4000 cm^{-1} is the tail of the large O-H stretching fundamental vibration near 3400 cm^{-1} (Small, 2006), the transition type for all radiation types are shown in table 4.

After irradiating the compound of interest, bonds of the molecule absorb the radiation resulting in a transition between two vibrational energy levels (v1 and v2). This

absorption occurs when the radiation energy equals the vibration energy. Not all vibrations are Infrared active; only those that exhibits a change in dipole moment are Infrared active (Banwell, 1972).

Table 4: The electromagnetic radiation characteristics.

Radiation Type	Radiation Source	Type of Transitions
Gamma rays	Gamma emitting radionuclides	Change in internal energy state of nuclei
X-rays	Synchrotron radiation	Inner electron
Ultraviolet	Deuterium lamp	Outer electron. Electronic transitions,
Visible	Tungsten lamp	Vibrational fine structure
Near-Infrared	Tungsten, dye laser	Outer electron molecular vibrations. Vibrational transitions, rotational fine structure
Infrared	Nerst glower, Globar, Xe, Ar, Discharge lamp	Outer electron, molecular vibrations. Vibrational transitions, rotational fine structure
Microwaves	Thermal	Molecular rotations, electron spin flips*, Rotational transitions
Radio waves	Oscillating conducting electrons	Nuclear spin flips*

Key: *Energy levels split by a magnetic field. IR region is of interest for this study.

At room temperature nearly all molecules exist in the vibrational ground state according to the Maxwell-Boltzmann law. Therefore, the three most important transitions in Infrared Spectroscopy are: $v = 0 \rightarrow v = 1$ ($\Delta v = 1$), $v = 0 \rightarrow v = 2$ ($\Delta v = 2$), and $v = 0 \rightarrow v = 3$ ($\Delta v = 3$). The first transition is called the fundamental absorption, the second and third are called first and second overtone respectively (Banwell, 1972; Swierenga, 2000). The vibration of molecules can be described using the harmonic oscillator model, by which the energy of different and equally spaced levels can be calculated from Equations 1 and 2.

$$E_{vib} = (v + \frac{1}{2}) \frac{\hbar}{2\Pi} \sqrt{\frac{k}{\mu}}$$ Eq1

Where v is the vibrational quantum number, $\hbar$ the Planck constant, k the force constant and μ the reduced mass of the bonding atoms, only those transitions between consecutive energy levels (Δv ± 1) that cause a change in dipole moment are possible,

$$\Delta E_{vib} = \Delta E_{rad} = \hbar v$$ Eq2

Where υ is the fundamental vibrational frequency of the bond that yields an absorption band in the middle IR region (Blanco and Villarroya, 2002), the harmonic oscillator model cannot explain the behaviour of actual molecules, as it does not take account of coulombic repulsion between atoms or dissociation of bonds (Blanco and Villarroya, 2002). As a result, the behaviour of molecules more closely resembles the model of a harmonic oscillator, the anharmonicity can result in transitions between vibrational energy states where Δv ± 2, Δv ± 3...these kind of transitions between non-continuous vibrational states yield absorption bands known as overtones (Blanco and Villarroya, 2002).

Spectra are characterized quantitatively by observing positive and negative peaks, which occur at specific wavelengths and quantified statistically to determine constituents of target materials such as soil and plant (Viscarra et al., 2006).

Shepherd and Walsh (2007) suggests that Infrared (IR) Spectroscopy can play a pivotal role in making the surveillance framework operational, by providing a rapid, low cost and highly reproducible diagnostic screening tool and noted the already usage of IR

Spectroscopy in the design of soil surveillance systems, hence proposed the same for plants.

IR has a short coming in that a single atomic entity with no chemical bonds makes it difficult to make spectral measurements; also if compounds of interest are present at very low concentrations they may have small influence on the spectral signature (Ichami, 2005).

On the other hand, the advantages of IR spectrometers for spectral signatures collection override this disadvantage and include: (1) spectrometers for collection of spectral signatures are standard thus there is minimal variation between spectral measurements of same analyte taken from different laboratories; (2) the technique is rapid, low cost (No chemical required), straightforward and accurate (Reeves *et al.,* 1994; Shepherd and Walsh, 2002; Viscarra *et al.,* 2006; Ichami, 2005); (3) large numbers of samples can be analyzed in a short period of time (Janik *et al.,* 1998; Ichami, 2005); (4) samples in any state (solution, paste, powder and fibers) can be analyzed; (5) the method is environmental friendly since no chemical disposal complications; (6) spectral results have a higher degree of reproducibility compares with results obtained from conventional laboratory methods (Shepherd and Walsh, 2007).

2.6 Multivariate calibration

The American Society for Testing and Materials (ASTM, 1998) defines multivariate calibration in Spectroscopy as "a process for creating a model that relates sample properties to the intensities or absorbance's at more than one wavelength or frequency of a set of known reference samples," the practice has also been made available for

17

multivariate calibration in near Infrared (NIR) and mid Infrared (MIR) Spectroscopy (Swierenga, 2000).

The digitalization of the NIR and MIR spectra at different wavelengths results in many and highly correlated variables (Small, 2006), but generally there is no well-defined physical law (model) available to predict the product properties from the corresponding spectrum (Swierenga, 2000). To extract chemical and physical information from such spectra, statistical modelling techniques or multivariate calibration models, such as Multiple Linear Regression (MLR), Partial Least Squares (PLS) and Principal Component Regression (PCR) are often used (Swierenga, 2000; Small, 2006).

2.6.1 Partial Least Square (PLS)

Partial Least Squares (PLS) predicts a set of dependent variables from a (very) large set of independent variables (Swierenga, 2000) by relating and extracting useful information from spectroscopic data to quantitative information of the measured samples. To obtain a PLS calibration model, various samples covering the future sampling space are measured along with the quantitative parameter(s) of the corresponding samples (Small, 2006).

These quantitative parameters are laboratory determined or calculated then a calibration model is developed to make predictions of the quantitative parameters when only the spectrum of a particular sample is measured (Small, 2006).

2.6.2 Principal Component Analysis (PCA)

Principal component analysis (PCA) is a mathematical procedure for resolving sets of data into orthogonal components whose linear combinations approximate the original

data to any desired degree of accuracy (Cozzolino *et al.,*2009). PCA procedure transforms a set of correlated variables into a smaller number of uncorrelated variables called principal components (or latent variables), orthogonal to each other (So *et al.,* 2004; Acuna, 2006). However, components are chosen to explain X (explanatory variables) rather than Y (response variables), and so, nothing guarantees that the principal components, which "explain" X, are relevant for Y (Abdi, 2003; Acuna, 2006).

2.7 The IR Model

2.7.1 Model development

The American Society for Testing and Materials (ASTM, 1998) describes standard steps for constructing, implementing, and maintaining a multivariate calibration model; these includes: 1) selecting calibration samples: 2) measuring properties and spectra of calibration samples: 3) calculating a calibration model: 4) validating the model: 5) applying the model for the analysis of unknowns: 6) monitoring the calibration model: and 7) updating the calibration model.

Although the process looks straight forward, this is not always the case as many sequential steps are usually involved in the building a calibration model, the steps include; rejection of outliers (both from the spectral and samples outliers) and spectral pre-processing.

The spectral pre-processing is usually necessary since: (1) some spectral regions may show a large variation not due to the parameter of interest (spectral region of interferent or spectral effect introduced by replacement of spectrophotometer or parts) (Swierenga,

19

2000): (2) spectral noise: (3) there may be wavelengths containing absorbance's that are not linearly related to the parameter of interest (Swierenga, 2000): (4) there may be wavelengths containing absorbance's that are not directly related to the parameter of interest but have an indirect correlation (apparent causalities) (Swierenga, 2000).

2.7.2 Model validation

The quality of the models in the calibration and prediction sets in IR- can be assessed using different criteria; the most common criteria are coefficient of determination (R^2), standard error of prediction (SEP) or cross validation (SECV), number of latent variables (LV) and ratio performance deviation (RPD), root mean square error of prediction (RMSEP) and the Bias.

The R^2 value is a measure of the variation of the response variable (wood density, carbon and nitrogen) explained by the regression model, while the SEC is a measure of the prediction error expressed in the units of the original measurement or SECV measures the efficiency of the calibration model in predicting the property of interest in a set of unknown samples differing from the samples that form the calibration set (Schimleck *et al.*, 2001). These parameters are given by;

$$R^2 = \frac{SSR}{TSS} \quad ....Eq3$$

$$RMSEP = \sqrt{\sum_{i=1}^{N_p} \frac{(\hat{y}_i - y_i)^2}{N_p}} \quad ....Eq4$$

$$SECV = \sqrt{\sum_{i=1}^{N_p} \frac{(\hat{y}_i - y_i)^2}{N_p - 1}} \quad \text{..Eq5}$$

$$Bias = \sqrt{\sum_{i=1}^{N_p} \frac{(\hat{y}_i - y_i)^2}{N_p - 1}} \quad \text{..Eq6}$$

Equations (3-6) are from Schimleck *et al.* (2001).

Where SSR is the sum square of regression, TSS is the total sum of squares, $\hat{y}_i$ are the predicted values, y_t measured reference values and N_p the number of samples to be tested.

2.8 Spectral pre-processing

Spectral pre-processing is applied to extract the descriptive information from the spectral data and to remove the non-descriptive information, examples are baseline drifts (linear or polynomial) and wavelength shifts, multiplicative signals and noise (Defo *et al.*, 2007; Swierenga, 2000).

The spectra pre-processing helps in the development of more simple and robust models, pre-treatment techniques used for spectra includes; normalization, derivatives (usually first or second), the multiplicative scatter correction (MSC), the standard normal variate (SNV), de-trending or a combination of all (Defo *et al.*, 2007). Table 5 outlines the effect of each pre-processing techniques, the techniques have proven to reduce the influence of effects such as baseline drifts (first and second derivative), multiplicative and additive effects caused by different particle sizes (multiplicative signal correction; MSC), non-

relevant information (wavelength selection), wavelength shifts and slope variation in a

spectrum (standard normal variate transformation; SNV) (Swierenga, 2000).

Every data pre-processing technique has its own specific properties and should,

therefore, be used to remove the spectral effect for which it has been designed for. An

example is a first derivative which is not capable to correct for wavenumber shifts

(Swierenga, 2000).

Table 5: Spectral data pre-processing techniques.

Pre-processing technique	Spectral effect
Mean Centering	Reduction of model complexity
Normalization	Removal of multiplicative effects
Standard normal variate (SNV)transform	Removal of additive and multiplicative spectral effects
Multiplicative signal correction(MSC)	Correction of additive and multiplicative spectral effects
First derivative	Removal of additive baseline
second derivative	Correction of sloped baseline
Variable selection	Removal of unimportant variables
Savitzky Golay smoothing in combination with derivatives	Noise reduction, additive and sloped baseline correction
Variance scaling	Equal contribution of all variables to model
Auto scaling	Mean centering and variance scaling
Logarithmic transformation	Normalization of variable distribution
Finite impulse response(FIR)	Correction of local additive and local multiplicative spectral effects
Kubelka-Munck transformation	Linearization of spectral variables
Fourier transform (FT)	Noise reduction and variable reduction
Wavelet transform (WF)	Noise reduction and variable reduction
Shift correction	Correction of wavelength shifts in spectral data
Principal component analysis (PCA)	Variable reduction, removal of noise, and visualization of data

Source: Swierenga (2000).

2.9 NIR and Multivariate analysis on wood

Quantitative analysis in IR Spectroscopy is based on multi-component form of the Beer-Lambert law, NIR Spectroscopy on wood involves measuring the reflectance of IR radiation between 12000 to 4000 cm^{-1} (Osborne *et al.*, 1993) and employing statistical methods such as principal components regression (PCR) or partial least squares regression (PLS) to find a few linear combinations of the original X-variables and to use only these components in regression equations (Small, 2006).

Principal components are created in a way that the first PC accounts for the maximum variation in the original data, the second PC accounts for as much of the remaining variance as possible, and so on. Only the most relevant part of the X-variation is used for regression as explained by highest percentages explained by the PCs (Naes *et al.*, 2002; Small, 2006).

Models are first calibrated using samples with known/measured parameters. Once the calibration models have been developed, prediction of these parameters is possible with new samples using only the NIR spectra and the calibration models. Successes have been shown in predicting wood density of softwoods. Hoffmeyer and Pedersen (1995) produced a density prediction model with a coefficient of determination of prediction R^2 greater than 0.90 while working with Norway spruce (*Picea abies*); on the same species, Thygesen (1994) used shavings to estimate the basic wood density.

Air-dry density of *Pinus taeda* was used by Schimleck *et al.*, (2003) to develop calibration equations using NIR spectra. A good prediction equation between NIR spectra and density of European larch wood (*Larix decidua*) was developed by Gindl *et*

23

al. (2001). Many studies applying NIR Spectroscopy to estimate wood properties have generally been based on solid wood samples of single species such as *Picea abies* (Thygesen, 1994; Hoffmeyer and Pedersen, 1995), *Eucalyptus delegatensis* (Schimleck *et al.,* 2001), *Pinus radiata* (Schimleck *et al.,* 2001) and *Eucalyptus globulus* (Schimleck *et al.,* 1999; Schimleck and French, 2001).

Recently Schimleck *et al.* (2001) developed a calibration for diverse range of species demonstrating wide densities and found out that some species, such as *Chlorophora excelsa* and *Daniellia ogea*, did not fit the calibration as well as the other species and this was attributed to the high extractives contents of these samples.

2.10 Application of multivariate analysis on MIR spectra

MIR seems to be valuable in following the molecular conformational changes, since the band shape reflects the degree of order in the system; it is easy to interpret the spectra and has been preferred to characterise the composition of agricultural products (Shepherd and Walsh, 2007).

The combination of MIR and multivariate data analysis techniques such as principal component (PCA) or discriminant analysis opens the possibility to unravel and interpret the spectral properties of the sample and allow qualitative analysis of the samples, such as discrimination or classification (Cozzolino *et al.,* 2009). This enhances the ability to build a characteristic spectrum that represents the finger print of the sample.

24

The ability of the MIR model to discriminate or identify wood core samples is based on the vibrational responses of chemical bonds to the electromagnetic radiation of MIR region (Cozzolino *et al.*, 2009). Therefore, it follows that the higher the variability between sample-types in those chemical entities corresponding to MIR regions of the spectrum, the better the accuracy of the model. The holistic compositional characteristic of the wood matrix provides the required information. However, the application of MIR in wood analysis is not fully exploited.

2.11 Methods of estimating wood density

Wood density is an important variable needed to obtain accurate estimates of biomass, carbon flux and greenhouse-gas emissions from land-use change (Nogueira, 2008). It is defined as the mass of oven-dry wood per unit of volume of green wood and expressed in grams per cubic centimetre or kilograms per cubic meter.

Wood density has a correlation with a number of plant functional traits and acts as an important indicator of the mechanical properties of woods (Chave *et al.*, 2009; Nock *et al.*, 2009). The density varies within the plant, during the plant life, and between and within individuals of the same species, among and within individual trees of a given provenance (Zobel and Van Buijtenen, 1989). The branches and the outer part of the trunk tend to have a lighter wood than the pith (Chave *et al.*, 2009). With each tree having its own characteristic wood density (O'Sullivan, 1976), the variation among different species is expected due to differences in anatomical structures.

Other factors that influences the variation of wood density includes: heritability whose expression is site specific as well as population specific, density being a highly heritable characteristic (Cown *et al.,* 1992). Because of anisotropic effect of wood's strength, it has different properties in longitudinal and tangential directions due to its cellular structure and physical organisation of the cellulose chain within the cell walls (Treacy *et al.,* 2000).

Linear relationship exists between strength and specific gravity (Treacy *et al.,* 2000). Wood moisture content among others affects wood density, thus it is usually expressed in one of the following ways: green (with the same moisture content as in the living tree), oven-dry (after heating in an oven at 105 C until constant mass is achieved), or air-dry (at equilibrium with ambient conditions or other specified conditions) (Williamson and Wiemann (2010). Thus density values for a given sample may vary depending on how it was analysed (Desch and Dinwoodie, 1996). Wood density is considered to be one of the most important wood properties which impacts on the freight costs, chipping properties, and pulp yield per unit mass of wood and paper quality (Schimleck *et al.,* 1999; Pliura *et al.,* 2007; WU Shi-jun *et al.,* 2010).

Measuring wood density from live trees can be expensive and time consuming, Several methods exist on wood density determination but quite a number are influenced by the method used in extracting samples from the trunk and how the volume of the sample is determined (Francis, 1994).

Indirect methods including penetrometer and SilviScan which uses a combination of X-ray densitometry, X-ray diffractometry and image analysis have been used (Shimleck,

2005). Extracting samples for wood density, carbon and nitrogen determination comes with challenges; the increment borer which has wide application in samples collection from living trees has a drawback of being expensive and borers with smaller diameters compresses the samples. Francis (1994) introduced a non-destructive method using a carpenters auger involving coring of tree trunk to collect cores at tree breast height and then safely estimate whole-tree density. However, to date the potential of this method is not exploited.

2.12 Predicting tree carbon and nitrogen

Determination of the role forests play in mitigating atmospheric carbon dioxide content globally is an important aspect; it is essential to have accurate inventory data of carbon content in forest organic matter (Lamlom and Savidge, 2003). The basic starting point is the tree wood; it represents the dominant pool of carbon. Carbon occurs in innumerable forms within forest ecosystems (Lamlom and Savidge, 2003).

Future policies for carbon sequestration in agriculture, forestry and landscape monitoring would require the measurement of carbon across species over time and at different geographical locations in order to determine whether, and if so, how much, carbon is being sequestered or lost from landscapes. Recent emphasis has been placed upon the ability to more accurately and precisely measure the carbon that is stored and sequestered in forests (Brown, 2002).

Near-Infrared reflectance Spectroscopy has become dominant method for analysis of agricultural products where large numbers of samples are used. In addition the technique

has been applied previously in soil carbon analysis (Madari *et al.*, 2005; Shepherd and Walsh, 2007). The limitation of Near-Infrared Spectroscopy is that it measures only organic carbon and is also known to be prone to biases (Madari *et al.*, 2005): Other standard methods for carbon analysis are: (1) the combustion or chromate oxidation (Madari *et al.*, 2005). (2) loss-on-ignition which is relatively cheap and rapid but suffers from accuracy problems, because mineral fractions can also be decomposed by heating (Madari *et al.*, 2005).

Both these methods require more than one determination in order to acquire information on both organic carbon and inorganic carbon (carbonates) and are not capable of determining other forms of carbon, such as soluble carbon, lignified carbon, charcoal and black carbon (Madari *et al.*, 2005). On the other hand, NIR requires only the development of calibrations then from a single spectrum all these parameters can be analysed.

Among other factors, two correlating variation in wood carbon content have been identified by Lamlom and Savidge (2003). First, the lignin content, species with high lignin content tend to display high carbon content. The second factor is the volatile carbon fraction in wood; this may contribute substantially to variation in total wood carbon content.

Thomas and Malczewskia (2007) reported data on the mass density and carbon content of tree organs, and in particular stem wood, are essential for accurate assessments of forest carbon sequestration. Dominant carbon pool within forest ecosystems is represented by wood (Lamlom and Savidge, 2003).

With few research data sets available on carbon content in woods, a default concentration of 50% (w/w) has been assumed and widely adopted, however, the value varies over a range of 47–59% depending on the species and soil type (Lamlom and Savidge, 2003). This could be due to uniqueness of wood chemistry as well as anatomy. Several studies have documented the potential of MIR to successfully predict carbon and nitrogen and other constituents of soils and different kinds of organic matter (Chang and Laird, 2002; Ludwig *et al.*, 2002; McCarty *et al.*, 2002; Michel *et al.*, 2006; Rossel *et al.*, 2006; Shepherd and Walsh,2007).

Although MIR is not as well established as NIR for the predictions, it may be more useful since intense fundamental vibration dominate the mid-IR region (Ludwig *et al.*, 2008). The MIR region is considered energetic enough to excite molecular vibrations to higher energy levels (Chalmers and Griffiths, 2002); the high selectivity of the MIR method makes the estimation of an analyte in a complex matrix possible. Interacting vibrations in these region gives rise to unique fingerprints for each compound (Banwell, 1972).

2.13 NIR and mineral content of plants

NIR can accurately estimate the content of several organic components in plants, crude protein, neutral detergent fibre, acid detergent fibre, cellulose, as well as other related parameters (Petisco *et al.*, 2005). There has been a controversy on the use of IR technique to determine the mineral content of plants; since most elements would not be expected to produce absorption in this region, except for rare earth elements such as holmium and didymium (Petisco *et al.*, 2005). Givens and Deaville (1999) reported the

usage of NIR in the determination of the concentration of certain cations owing to their association with organic or hydrated inorganic molecules.

Calibration model was also developed by Batten and Blakeney (1992) to estimate N, S, P, K and Mg contents in dry ground rice shoot samples by examining the influence of inter-correlations between constituents on the true ability of NIR to determine mineral nutrients (Petisco *et al.,* 2005).

CHAPTER THREE

MATERIALS AND METHODS

3.1 Study Site

The study was conducted in Yala basin which had three blocks: Middle Yala, Lower Yala and Upper Yala (Figure 2). The study sites were previously identified by the Western Kenya Integrated Ecosystem Management Project (WKIEMP) and covers Siaya district in Nyanza and Western province (Boye *et al.*, 2008).

The three blocks measured approximately 100 km^2 and were characterized by low crop productivity together with land degradation. The annual rainfall ranges from 1200 mm to 1800 mm in western and between 800 to 1900 mm in Siaya; annual mean temperature is 28°C.
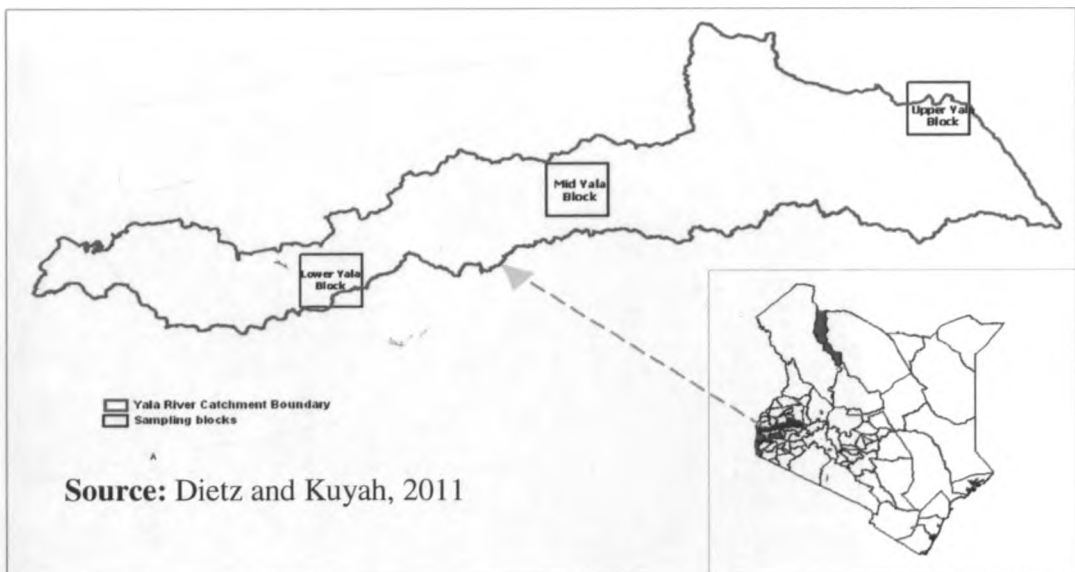
Figure 2: Yala river basin with the three blocks.

3.2 Sample collection

Coring through the bark to the start of the heartwood (as noted by a colour change) was done at constant height of 1.3 m above the ground, diameter at the breast height (DBH) (Figure 3), 10 cm above DBH (R1) and 10 cm below DBH (R2) the first chips produced in coring the preparatory hole was discarded. This cored hole through the bark was brushed out and its depth measured with a ruler. This became the starting depth of the sample; three cores were taken per tree trunk; root and branch cores were also taken in addition.

Short cylindrical cores, approximately 30–100 mm long (depending on tree diameter) from the periphery into the inner portion of the trunk were obtained using a 2.5-mm-wide carpenters auger bit, upon withdrawal of the auger, chips remaining in the hole were collected using a flattened stick or thin spatula and added to the sample collection plastic bag.

Figure 3: Tree core sampling using carpenter's auger.

Tree cores were selected to include a broad range of species from middle Yala, lower Yala and upper Yala, although, the number was limited. Selection was random representing full range of diameters classes of the present trees on farm.

3.2.1 Samples preparation

Fresh weight of each core sample was taken in the field and then placed in a zip lock bag for transportation to the laboratory where they were dried at 105°C in oven until no further weight loss. Weights were taken after oven drying and recorded. Cores were ground and sieved using a sieve size of 0.5 mm into a fine powder and placed in zip lock bags.

3.3 Wood density calculations-coring method

Cored volume (v) was determined by assuming the core is cylindrical and hence using

$$v = \frac{\Pi d^2}{4} \times h$$

....Eq7

Where, d is the bit diameter (2.5 cm) and h, is the core depth in cm.

Relative wood density (w_d) or specific gravity in g cm^{-3} was then calculated as the ratio of wood dry mass (d_m) to core volume (v).

$$w_d = \frac{d_m}{v}$$

....Eq8

Where, d_m is wood dry mass (gms) and v is core volume.

3.4 Carbon and nitrogen analysis

2 mg of fine ground samples were placed in tin capsule (Analytical Technologies Inc., Valencia, CA, USA) then analyzed for carbon and nitrogen using a CN analyzer Thermo-Quest Flash EA1112 according to manufacturer's protocol.

3.5 NIR Spectroscopy measurements

A 5 g portion of fine ground cored sample was put in clean labelled glass vial then mixed for homogeneity. Two scans for near Infrared were generated then averaged. Cored samples were scanned through the bottom of the glass vial placed on an integrating sphere window.

Spectral data was collected in reflectance mode using a high intensity contact probe attached to Fourier Transform Infrared Multi-purpose Analyzer (FTIR MPA) (Figure 4) between 350 to 2500 nm (12000-4000 cm^{-1}). FTIR was found in ICRAF spectral laboratory in Nairobi. For each spectrum, 30 scans were collected by the spectrometer and averaged to produce a single spectrum.

Figure 4: Bruker Transform Infrared multi-purpose Analyzer

3.6 MIR-Spectroscopy measurements

Another set of fine ground samples (approximately one gram) were loaded into 96 well aluminium micro titre plates (Figure 5) with an empty cell used as background reference. The plant samples were then analyzed in the Mid-Infrared (4000 – 600 cm^{-1}) diffuse reflectance region using a Bruker High-Throughput-Screening (HTS-XT) accessory attached to a Bruker Tensor 27 FT-IR spectrometer.
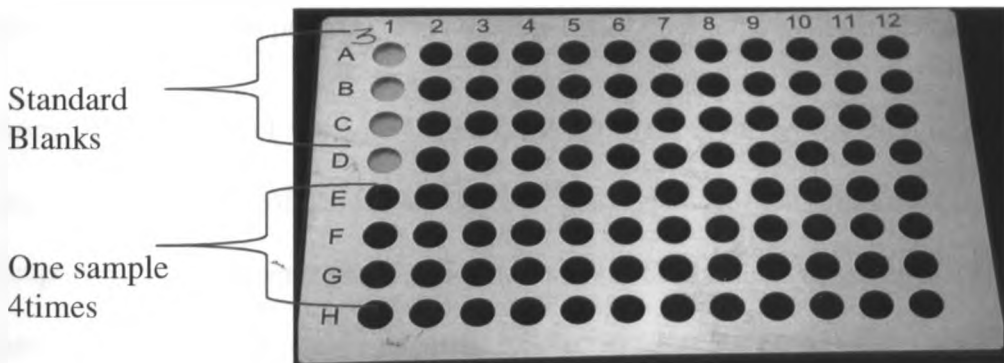
Figure 5: Aluminium micro plate used to scan cored samples.

3.7 Pre-processing of spectra

IR spectra of wood samples are generally influenced by the physical properties of the samples (Defo *et al.*, 2007). To minimize these contributions that incorporate irrelevant information into spectra, first derivative spectral pre-treatment method was used.

3.8 Infrared Calibration

3.8.1 Calibration samples selection from IR spectra

The selection of representative calibration samples IR analysis were selected based on recorded NIR and MIR spectral diversity using the Kennard-Stone algorithm and calculated principal component scores. Kennard-Stone algorithm procedure consists of selecting as the next sample (candidate object) the one that is most distant from those already selected objects (calibration objects). The distance is usually the Euclidean distance although it is possible, and probably better, to use the Mahalanobis distance.

From the spectra of all 404 core samples, the approach involved selection of calibrations sets based on variety of sample set designs; these include: (1) Calibrations based on all samples with no independent validation/test set. (2) Calibrations based on a 50/50 split of samples. (3) Calibrations using 10%, 20%, 30%, 40%, 60%, 70%, 80%, 90% in calibration set in which every remaining sample was used as the validation set respectively. (4) Using only *E. camaldulensis* as calibration set given that it was most abundant in the blocks. Calibrations were then developed using each spectral range of NIR and mid-IR.

3.8.2 IR prediction model

The construction of the prediction model followed the following key processes: 1)
Scanning and recording IR spectra of samples. 2) Choosing the calibration samples using
PCA analysis of spectra. 3) Determining the target parameter on selected samples by
using the reference method. 4) Subjecting spectra to appropriate pre-treatments. 5)
Predict the know samples constituents with the developed model. 6) Validating the
model and predicting unknown samples as illustrated in summary model diagram in
Figure 6.
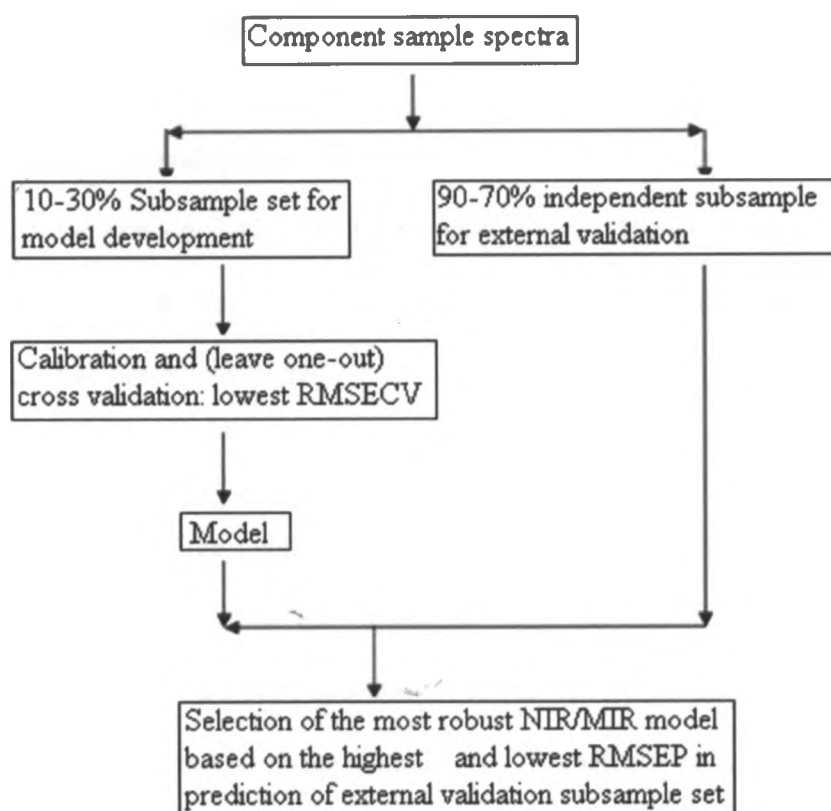
Figure 6: Summary model in the calibration model-construction.

3.9 Data analysis

3.9.1 Field data

Exploratory data analysis was done using GenStat statistical software (Payne *et al.*, 2009) and XLSTAT version 2008.6 to understand the interactions between densities with tree parts and species Tukey's test was carried out on mean separation for the different tree parts. Pearson correlation coefficient was used estimate strength and direction of association between wood density and carbon.

3.9.2 Multivariate analysis

Calibration development was done using PLS regression statistical analysis using R software version 2.12.1 (R Development Core Team, 2008) available from www.r-project.org. Validation of the calibration model was carried out using "leave-one-out" cross-validation technique.

The Predicted Residual Error Sum of Squares (PRESS) was computed from the error in prediction from the standards by cross-validation and plotted as a function of the number of factors employed in the calibration; Spectral information was within the range of 8000-4000 cm^{-1} for NIR and 600–4000 cm^{-1} (~18,000–2500 nm) for MIR. The spectra were merged into a single data matrix (X-matrix) while wood density, carbon and nitrogen data were combined into a response matrix (Y-matrix).

3.9.3 Partial Least Square (PLS) analysis

The data set was divided into calibration sets for developing discriminant models and prediction sets for evaluating the classification performance of the computed models. Multivariate analysis of the spectroscopic data was made through the use of the R statistical software.

PLS regression was used to develop the calibrations with a cross validation method, factors that produced the highest coefficient of determination (R^2) in the prediction set was used, very high coefficient of determination in a model can result to over fitting with a high number of latent variables resulting to poor performance of prediction when the model is used with the prediction set. Thus the quality of the models in the calibration and prediction sets was measured with R^2 and error evaluation done using root mean square error of prediction (RMSEP) (Martens and Naes, 1991; Acuna, 2006). The RMSEP shows how far typical points are above or below the regression line.

CHAPTER FOUR

RESULTS AND DISCUSSION

4.1 Wood cores

A total of twenty different species found on-farm were selected. Middle Yala had the highest number of species both indigenous and exotic while in Upper Yala no indigenous tree was found (Table 6).

Table 6: Total Species collected from Yala Basin.

Site	Indigenous species	Exotic species
Middle Yala	*Bridelia micrantha*	*Cuppresus lusitanica*
	Croton macrostachyus	*Eucalyptus camaldulensis*
	Harungana madagascalensis	*Eucalyptus grandis*
	Markhamia lutea	*Eucalyptus saligna*
	Prunus africana	*Mangifera indica*
	Syzygium cordatum	*Persia americana*
	Trilepisium madagascariensis	*Syzygium cuminii*
Upper Yala	No Indigenous species	*Acacia mearnsii*
		*Cupressus lusitanica**
		*Eucalyptus grandis**
		Grevillea robusta
		Jacaranda mimosifolia
Lower Yala	*Combretum molle*	*Grevillea robusta**
	Ficus spp	*Mangifera indica**
	*Markhamia lutea**	*Syzygium cuminii**
	Spathodea campanulata	

Key*=Repeated species in other sites

4.1.1 Lower Yala

Lower Yala had 4 indigenous and 3 exotic species as shown in table 7 from which 69 cores were taken at different tree positions, this included DBH, R1 and R2, Branches and Roots. The frequency of each tree part sampled varied are shown (Figure 7, Figure **8** and Figure **9**). *Mangifera indica* had the highest number of cores since it was the most common in the area (46.38%) followed by *Markhamia lutea* at 20.29% and *Spathodea campanulata* at 4.35%.

Table 7: Total number of individual species collected from Lower Yala.

Species	Number of cores	Number of individual species
Combretum molle	5	1
Ficus spp	5	1
Grevillea robusta	5	1
Mangifera indica	32	6
Markhamia lutea	14	5
Spathodea campanulata	3	1
Syzygium cuminii	5	1
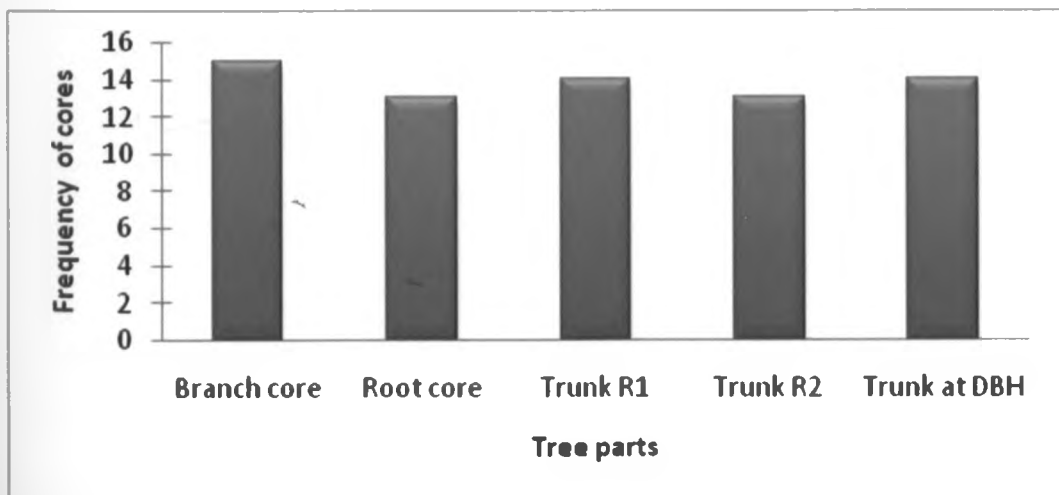
Figure 7: Frequency of tree parts cored in Lower Yala.

Among the most sampled tree parts across the species in this region, branch cores had the highest frequency of 15 equivalents to 21.74% followed by Trunk R1 and Trunk at DBH both having 14 (20.29%). Root core and trunk replicate (R2) were both at 18.84%.

4.1.2 Middle Yala

A total of 252 cores from 14 different species found in this area were collected (Table 8). *Eucalyptus camaldulensis* had the highest number of cores representing its abundance in the area with 119 cores recorded representing 47.22% of entire samples collected. This was followed by another *Eucalyptus species, Eucalyptus grandis* at 11.51%, with *Croton macrostachyus* at 1.19% being least sampled.

Table 8: Total number of individual Species collected from Middle Yala.

Species	Number of cores	Number of individual species
Bridelia micrantha	7	2
Croton macrostachyus	3	2
Cupressus lusitanica	15	4
Eucalyptus grandis	29	7
Eucalyptus camaldulensis	119	28
Eucalyptus saligna	6	6
Harungana madagascariensis	5	1
Mangifera indica	5	1
Markhamia lutea	16	4
Persea americana	7	2
Prunus africana	20	16
Syzygium cordatum	10	2
Syzygium cuminii	5	1
Trilepisium madagascariensis	5	1

The distribution frequency on tree parts sampled (Figure 8) was high for Trunk at DBH (74%) while branch core was at 35%.
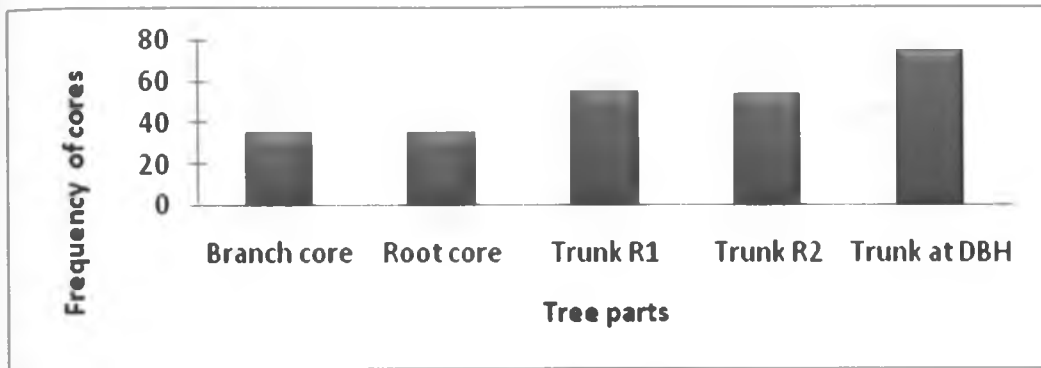
Figure 8: Frequency of tree parts cored in Middle Yala.

4.1.3 Upper Yala

Acacia mearnsii had the highest number of cores and most common species in the area with 36 cores representing 43.37% of the total 83 cores from this block. *Grevillea robusta* at 27.71% and *Cupressus lusitanica* at 3.61% (Table 9). The frequency distribution of tree part cores across this block is shown in Figure 9.

Table 9: Total number of individual cores collected from Upper Yala.

Species	Number of cores	Number of species
Acacia mearnsii	36	7
Cupressus lusitanica	3	1
Eucalyptus grandis	10	3
Grevillea robusta	23	4
Jacaranda mimosifolia	11	2

The distribution frequency of Trunk at DBH, Trunk R1, Trunk R2 and branch cores were equal (18%), while Root core had the lowest frequency 11%.
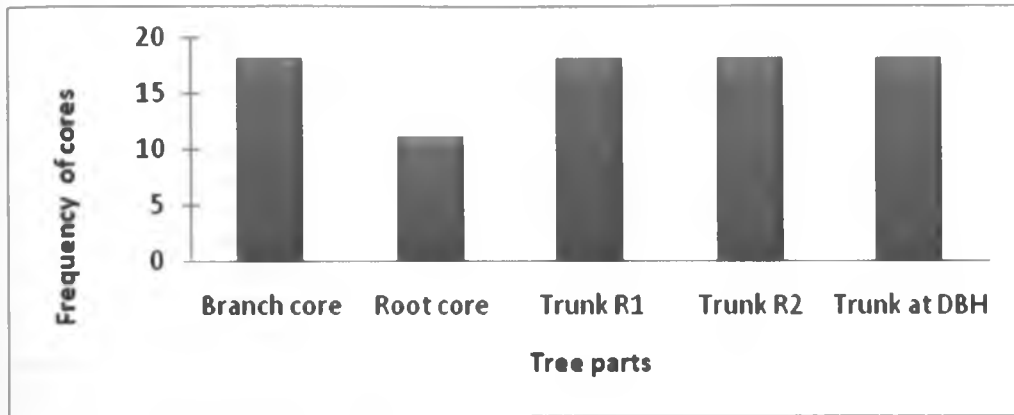
Figure 9: Frequency of cores from Upper Yala.

4.2 Wood densities

Density by species based on tree parts (Trunk, Roots and Branches) cored was explored using box plots (Figure 10, Figure 11 and Figure 12). Box plots are useful when comparing two or more sets of sample data by giving a picture of the symmetry of a dataset, and shows outliers very clearly. From the box plots, outliers were removed before averaging cores from different tree parts in order to get whole tree density by species.

Note: Numbers besides boxes show outliers
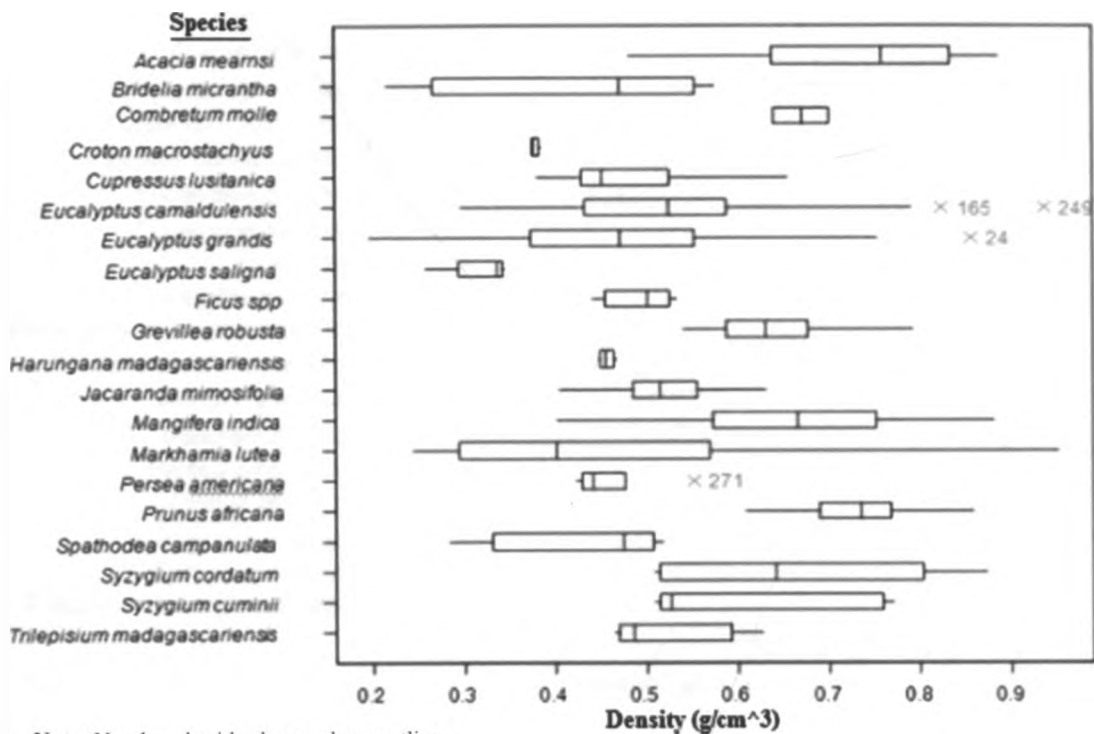
Figure 10: Box plot of wood density by species based on trunk cores.

Note: Numbers besides boxes show outliers
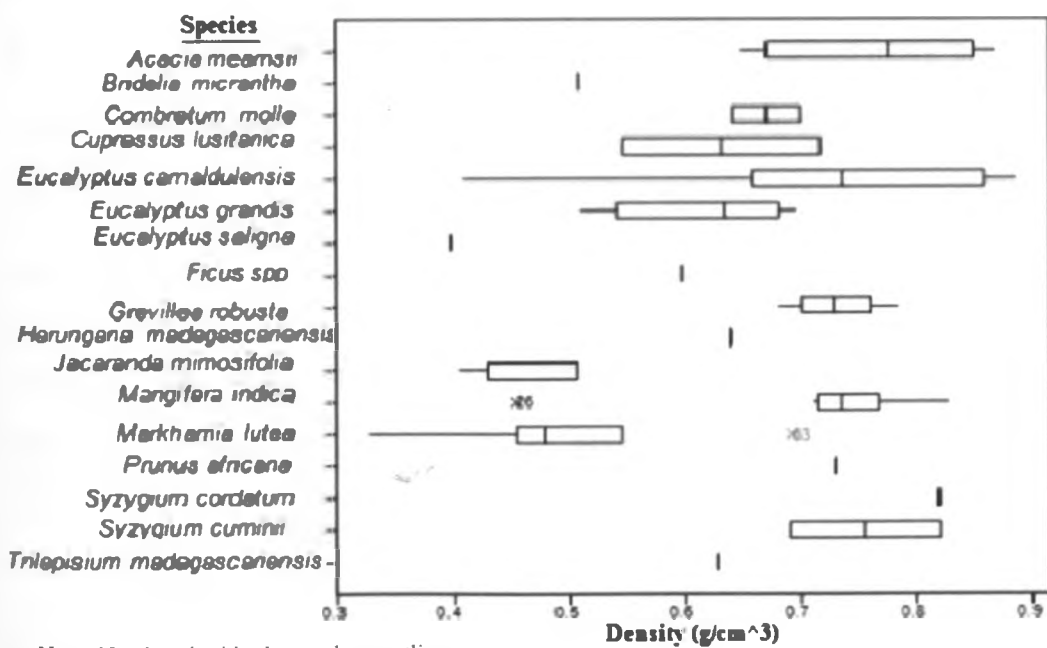
Figure 11: Box plot of wood density by species based on branch cores.

46
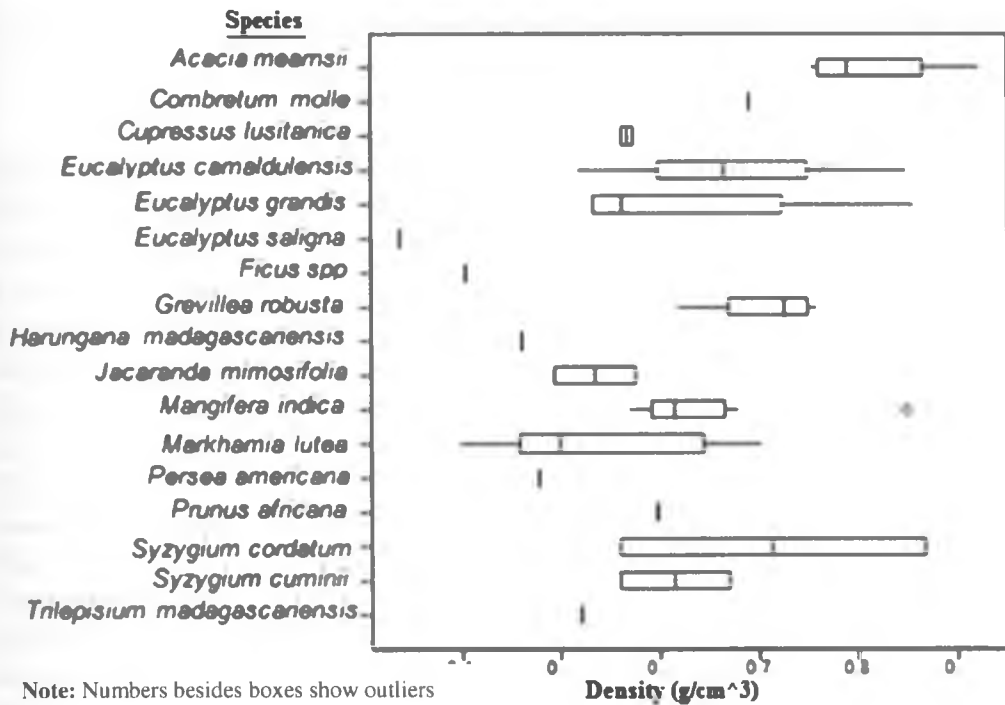
Figure 12: Box plot of wood density by species based on Root cores.

4.3 Whole tree density

Before averaging the densities, means of tree parts were separated using Tukey's mean separation (Table 10) using GenStat Statistical software (12th edition); The means were not significantly different at p=0.05. Whole tree densities of species from the three blocks calculated from carpenter's auger method are summarized in table 11.

Table 10: Tukey's mean separation of tree parts

Tree part	Mean
Root core	0.4877
Trunk R2	0.5295
Trunk at DBH	0.5359
Trunk R1	0.5430
Branch core	0.5445

Note: Means are not significantly different at p=0.05

Table 11: Whole tree densities of species from the Yala Basin

Species	TS	Tc	Mean (gcm^{-3})	Min (gcm^{-3})	Max (gcm^{-3})	Variance	S.d
Acacia mearnsii	7	31	0.66	0.47	0.81	0.01	0.08
Bridelia micrantha	2	7	0.38	0.22	0.55	0.02	0.13
Combretum molle	1	5	0.66	0.58	0.70	0.00	0.05
Croton macrostachyus	2	3	0.44	0.38	0.56	0.01	0.11
Cupressus lusitanica	5	18	0.48	0.36	0.66	0.01	0.09
Eucalyptus camaldulensis	28	108	0.51	0.30	0.79	0.01	0.11
Eucalyptus grandis	10	37	0.47	0.22	0.75	0.01	0.12
Eucalyptus saligna	2	5	0.34	0.17	0.45	0.01	0.11
Ficus spp	2	5	0.44	0.28	0.53	0.01	0.10
Grevillea robusta	19	27	0.62	0.52	0.72	0.00	0.05
Harungana madagascariensis	2	4	0.47	0.45	0.49	0.00	0.02
Jacaranda mimosifolia	6	10	0.47	0.35	0.63	0.01	0.09
Mangifera indica	24	35	0.57	0.40	0.71	0.01	0.08
Markhamia lutea	13	29	0.41	0.20	0.69	0.02	0.13
Persea americana	3	5	0.44	0.42	0.48	0.00	0.02
Prunus africana	14	16	0.74	0.67	0.79	0.00	0.04
Spathodea campanulata	1	3	0.43	0.28	0.52	0.02	0.13
Syzygium cordatum	7	10	0.76	0.68	0.79	0.00	0.04
Syzygium cuminii	6	10	0.56	0.40	0.77	0.02	0.13
Trilepisium madagascariensis	3	5	0.52	0.45	0.68	0.01	0.09

Key: SD= standard deviation, TC=number of cores from each species, TS= Total number of species

A total of 373 cores from three blocks were used for wood density estimation after removing all the outliers; out of 404 core samples 31 outliers were removed from which root cores contained the highest number of outliers followed by branch core, indicating a possibility of a problem with branch and root coring during samples collection. Trunk had the least number of outliers.

The densities were in the range of 0.34–0.75 gcm^{-3} with an average mean value of 0.55 gcm^{-3}. *Eucalyptus saligna* was found with the lowest density value of 0.34 gcm^{-3} while

Syzygium cordatum had the highest density value of 0.75 gcm^{-3}. Within the same genus of *Eucalyptus*, density values ranged from 0.51-0.34 gcm^{-3} with *Eucalyptus camaldulensis* having the highest density value followed by *Eucalyptus grandis* at 0.47 g cm^{-3}.

A study by Rueda and Williamson, (1992) showed that pioneer trees grow quickly at first, producing low-density wood, and later add structural support by adding a shell of harder wood. The controlling factor for adding the harder wood is the age of the tree, rather than the diameter (De Castro *et al.,* 1993).

4.4 Interactions between densities with species and tree parts

The Interactions between densities with species and tree parts showed significant effect with F<0.001 for species as shown in table 12. However, there was no significance difference in density between tree parts and species.

Table 12: Interactions between densities with tree species and tree parts.

Change	DF	SS	MS	F pr
+ Species	20	3.308752	0.165438	<0.001
+ Tree parts	7	0.112910	0.016130	0.128
+ Species. Tree parts	69	0.504632	0.007314	0.934
Residual	276	2.735716	0.009912	
Total	~372	6.662010	0.017909	

Key: ms= means standard error, ss=sum of squares, DF= degrees of freedom

4.5 Calculated and reported densities

The reference Global Wood Density database (GWD), which has wood densities for 8412 species from around the world (Flores and Coomes, 2010), and the African wood

density database (Carsan *et al.,* 2012) provided data for comparison with the calculated density values using different methods. Wood densities of similar species reported from tropical Africa encountered in these databases were averaged, but since these densities are reported in units of mass of wood at 12% moisture content per unit of volume at 12% moisture content, a correction to equivalent oven dry densities was done using a calibration equation developed by Reyes *et al.* (1992) by multiplying reported values by 0.88. The databases provided an opportunity for comparison between the calculated density values and the reported densities (Table 13).

Table 13: Calculated densities and reported densities.

| Species | C.d | Reported densities (gcm^{-3}) by regions | | | | | |
		T. Africa	Astl	S-E Asia	China	SA	India
Acacia mearnsii	0.66	-	0.66	-	-	-	-
Bridelia micrantha	0.38	0.44-0.58		0.50		-	-
Combretum molle	0.66	0.79	-	-	-	-	-
Croton macrostachyus	0.44	0.45-0.52	-	-	-	-	-
Cupressus lusitanica	0.48	0.39	-	-	-	-	-
Eucalyptus camaldulensis	0.51	-	0.48-0.97	-	0.59	-	-
Eucalyptus grandis	0.47	-	0.63-0.66	-	-	-	-
Eucalyptus saligna	0.34	-	0.68-0.86	-	-	-	-
Ficus spp	0.44		-	-	-	-	-
Grevillea robusta	0.62	0.51-0.516	-	0.5	-		0.64
Harungana madagascariensis	0.47	0.47	-	0.47	-	-	-
Jacaranda mimosifolia	0.47	-	-		-	-	-
Mangifera indica	0.57	0.54	-	0.52	-	-	0.68
Markhamia lutea	0.41	0.47	-	-	-		
Persea americana	0.44	0.52	-	-	-	0.6	
Prunus africana	0.74	0.77	-	-	-	-	-
Spathodea campanulata	0.43	-	-	-	-	-	-
Syzygium cordatum	0.76	0.62	-	-	-	-	-
Syzygium cuminii	0.56	-	-	-	0.63		0.76
Trilepisium madagascariensis	0.52	0.50	-	-	-	-	-

Key: Cd= calculated density, T. Africa=Tropical Africa, Astl = Australia, SA=South America,-no reported value

From these two databases not all species were reported and the density of *Ficus spp* was not reported in the global data base; however most of the values reported were within the range of those calculated using the carpenter's auger method.

4.6 Carbon and nitrogen analyses

Total carbon and nitrogen concentrations determined using thermal oxidation are summarized in tables 14 and 15. Measured carbon and nitrogen values in percentage were converted to contents (gcm^{-3}) by dividing by 100 then multiplying by the corresponding species density.

Table 14: Measured carbon (%) and Carbon contents (gcm^{-3}).

Species	TS	Nc	Mean	Min	Max	Variance	S.d	C(gcm^{-3})
Acacia mearnsii	27	24	48.08	47.36	48.61	0.14	0.37	0.32
Bridelia micrantha	3	7	45.02	43.95	45.99	0.40	0.63	0.17
Combretum molle	3	5	46.80	45.49	48.05	0.86	0.93	0.31
Croton macrostachyus	1	3	44.13	43.95	44.44	0.07	0.27	0.20
Cupressus lusitanica	9	15	47.21	46.19	48.67	0.44	0.67	0.23
Eucalyptus camaldulensis	63	116	46.50	44.61	48.54	0.74	0.86	0.24
Eucalyptus grandis	10	37	48.37	46.90	50.31	0.64	0.80	0.23
Eucalyptus saligna	6	6	47.97	45.13	49.41	2.72	1.65	0.17
Ficus spp	1	5	47.80	46.92	48.51	0.33	0.57	0.21
Grevillea robusta	5	22	49.17	47.31	50.68	0.78	0.88	0.30
Harungana madagascariensis	1	5	48.51	47.53	49.27	0.46	0.68	0.23
Jacaranda mimosifolia	2	11	48.60	46.04	50.02	1.61	1.27	0.23
Mangifera indica	7	36	47.19	45.60	48.60	0.45	0.67	0.27
Markhamia lutea	9	30	48.77	47.11	50.72	0.78	0.88	0.20
Persea americana	2	6	47.52	46.88	48.03	0.18	0.43	0.21
Prunus africana	16	20	47.93	46.50	49.14	0.50	0.71	0.35
Spathodea campanulata	1	3	47.43	46.25	48.46	1.24	1.11	0.20
Syzygium cordatum	2	9	48.23	47.31	49.08	0.35	0.59	0.37
Syzygium cuminii	2	10	48.56	45.61	51.26	2.06	1.43	0.27
Trilepisium madagascariensis	1	5	47.41	46.64	47.84	0.25	0.50	0.25

Key: SD= standard deviation, Nc=number of cores from each species, TS= Total number of trees, C=carbon content in gcm^{-3}.

Table 15: Measured Nitrogen (%) and Nitrogen contents (gcm^{-3}).

Species	TS	Nc	Mean	Min	Max	Variance	S.d.	$N(gcm^{-3})$
Acacia mearnsii	27	35	0.27	0.14	0.38	0.0049	0.07	0.0018
Bridelia micrantha	3	7	0.23	0.21	0.25	0.0001	0.01	0.0009
Combretum molle	3	3	0.29	0.28	0.31	0.0004	0.02	0.0019
Croton macrostachyus	1	3	0.27	0.26	0.28	0.0001	0.01	0.0012
Cupressus lusitanica	9	18	0.22	0.13	0.28	0.0016	0.04	0.0011
Eucalyptus camaldulensis	63	118	0.22	0.11	0.34	0.0016	0.04	0.0011
Eucalyptus grandis	19	31	0.20	0.11	0.42	0.0036	0.06	0.0009
Eucalyptus saligna	2	6	0.21	0.18	0.26	0.0009	0.03	0.0007
Ficus spp	2	5	0.30	0.29	0.31	0.0001	0.01	0.0013
Grevillea robusta	19	28	0.23	0.09	0.35	0.0025	0.05	0.0014
Harungana madagascariensis	2	5	0.25	0.23	0.28	0.0004	0.02	0.0012
Jacaranda mimosifolia	6	11	0.30	0.25	0.36	0.0009	0.03	0.0014
Mangifera indica	24	37	0.24	0.11	0.37	0.0016	0.04	0.0014
Markhamia lutea	13	28	0.34	0.24	0.43	0.0016	0.04	0.0014
Persea americana	3	7	0.25	0.21	0.31	0.0016	0.04	0.0011
Prunus africana	16	20	0.21	0.14	0.29	0.0009	0.03	0.0016
Spathodea campanulata	1	3	0.24	0.23	0.26	0.0004	0.02	0.0010
Syzygium cordatum	7	10	0.28	0.24	0.31	0.0004	0.02	0.0021
Syzygium cuminii	6	9	0.24	0.16	0.36	0.0036	0.06	0.0014
Trilepisium madagascariensis	3	5	0.29	0.21	0.32	0.0025	0.05	0.0015

Key: SD= standard deviation, Nc=number of cores from each species, TS= Total number of trees, N=Nitrogen content in gcm^{-3}

Species mean carbon values ranged from 44 to 49% and 0.17 to 0.36 g cm^{-1} for carbon content. The carbon and nitrogen values were in agreement with previously reported range, species variation in total C was statistically significant (P<0.001), with values ranging from 44.13% in *Croton macrostachyus* to 49.17% in *Grevillea robusta* (Table 14).

Carbon variation and measurement error was relatively low, with an average standard deviation of 0.79%. All the twenty species examined had an average percentage C of 47.56%, significantly lower than 50% default carbon value. Thus, this variation with thee often assumed default value of 50% C in wood could lead to an over estimation of tree C stocks but still provides a rough estimate of carbon biomass.

Most species deviated from this estimate by between 1-4% using 50% as reference value. *Croton macrostachyus* an indigenous species in the area showed high deviation of 4%. However, similar deviations of 2–3% among conifers were reported by Thomas and Malczewski (2007). For conifers, 2–3% deviation resulted in 4–6% bias in carbon stock assessments (Thomas and Malczewsk,i 2007).

The reported deviation of 1-4% in this study could result in about 2-8% bias in carbon stock assessments in tropical agricultural landscape. A 1% difference in carbon content conceivably could have a significant impact on wood and pulp industries in relation to allocation of carbon credits within the context of Kyoto Protocol (Lamlom and Savidge, 2003).

The total nitrogen concentration among different species ranged from 0.34% in *Markhamia lutea* to 0.2% in *Eucalyptus grandis*. Elemental nitrogen in plants has been

reported by Pettersen (1984) to be in the range of 0.1-0.5%. The twenty species had a mean value of 0.25% and range of 0.17 to 0.36 gcm^{-3} for nitrogen content.

4.7 Correlation between wood density, carbon and nitrogen contents

Wood density values were positively correlated with carbon content (r = 0.995) and nitrogen content (r = 0.849), these were supported by Pearson correlation matrix (Table 16 and Figure 13).

Table 16: Pearson correlation between density, carbon and nitrogen.

Variables	Density(gcm^{-3})	Carbon(gcm^{-3})
Carbon (gcm^{-3})	**0.995**	
Nitrogen(gcm^{-3})	**0.849**	**0.844**

Key: Values in bold are significantly different with a significance level alpha p < 0.05.

In general, there was a very strong positive correlation between wood density, carbon and nitrogen, all at p<0.0001. These correlations are important in carbon pool assessment and are in agreement with Dietz (2007) that a better understanding of wood density values can reduce the error of carbon pool estimation.

The higher the density values the higher the C and N contents (Figures 13 and 14). Hacke *et al.* (2001) showed that wood density correlates positively with carbon and concluded that high wood density is advantageous for survival in dry climates and may aid in the transport of liquids in dry conditions. However, this may suggest the adaptation of these species to the Yala basin given that wood tends to be chemically as well as anatomically unique for individual species. Therefore, it would be reasonable to

expect that each species would have characteristic carbon content (Lamlom and Savidge, 2003).
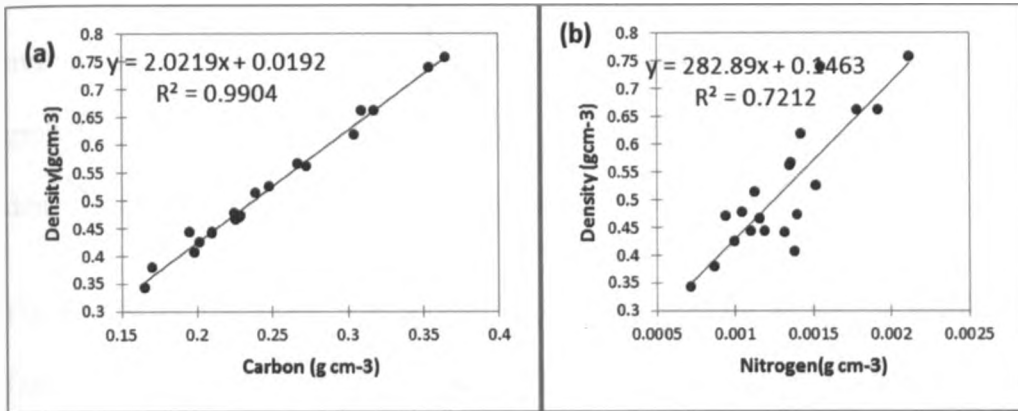
Figure 13: Correlation between 20 species for density (a) with nitrogen (b).
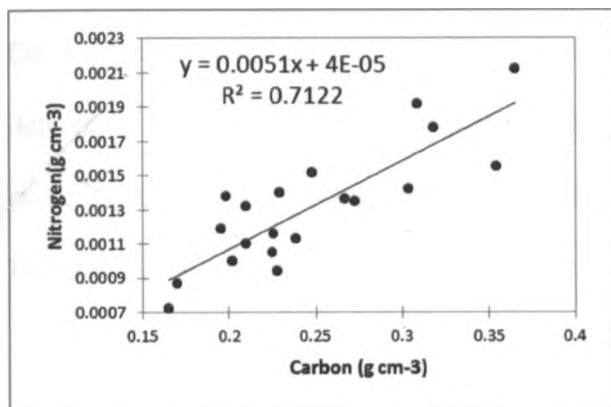
Figure 14: Correlation between nitrogen with carbon for 20 species.

Positive relationship among species on nitrogen and carbon contents exists as shown in Figure 14. Although the lignin to nitrogen ratio is known to change during decomposition, this study did not calculate the ratio of carbon to nitrogen which has an inverse correlation to lignin concentration; so the higher the ratio of carbon to nitrogen the lower the lignin concentration (Melillo *et al.*, 1982).

4.8 Species variation with wood density, carbon and nitrogen

High wood density is a characteristic of slowly growing species, found in dry soils or in nutrient-poor soils (Preston *et al.,* 2006; Muller-Landau, 2004) than similar shrub-like growth (Preston *et al.,* 2006). *Syzygium cordatum* and *Prunus africana* had highest densities (Note: Size of points indicates increasing densities.

Figure 15). *S. cordatum* is described in ICRAF database as one of southern Africa's fastest growing trees (up to 1m/year) while *Prunus africana* is described as a slow growing species.

Growing the same species in different geographical locations can result in readily detectable differences in wood properties. Some softwood species showed higher carbon content; which was attributed to the fact that softwoods have approximately 10% more lignin than hardwoods (Lamlom and Savidge, 2003).
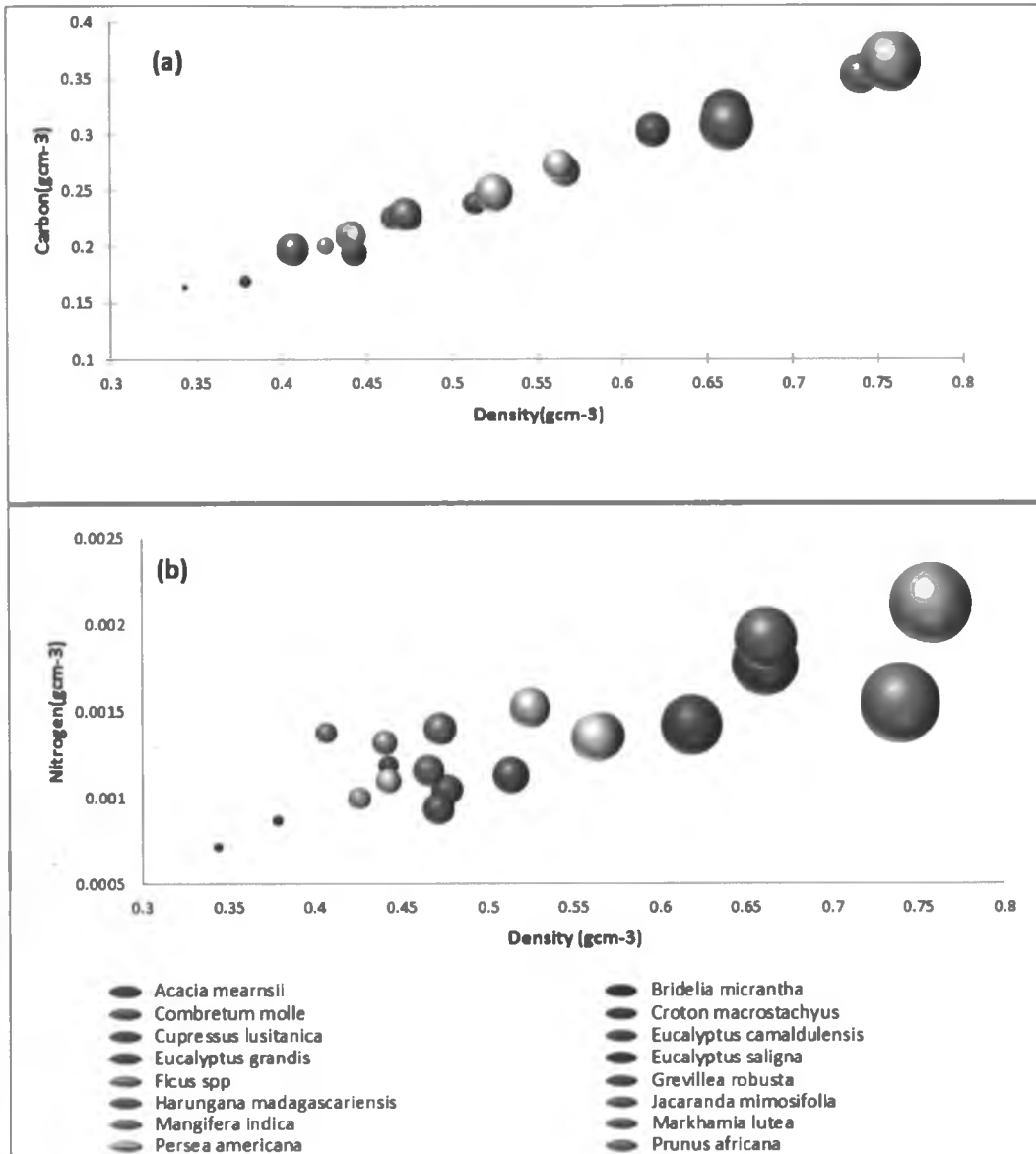
Note: Size of points indicates increasing densities.

Figure 15: Species-specific density values with (a) carbon (b) nitrogen

The kind of positive relationship (R^2=0.99) between wood density and carbon content (Note: Size of points indicates increasing densities.

Figure 15) are practically useful for C stock estimation since determination of carbon is relatively difficult and expensive (Elias and Potvin, 2003).

Wood density has been proposed as a good proxy to C estimation in tropical trees. Findings by Elias and Potvin, (2003) showed strong relationships between C and wood density (R^2 = 0.86). Similar relationship was reported by Thomas, (1996) and Muller-Landau, (2004) in diverse forest ecosystems. Theoretically slow-growing species often contain high C compounds (e.g., lignins, polyphenolic compounds), whereas fast-growing species contain low C compounds (e.g., alkaloids, phenolic glycosides, cyanogenic glycosides).

Schlesinger (1991) reported that C content of biomass is almost always found to be between 45% and 50% (by oven-dry mass) and thus, the carbon content of vegetation may be estimated by simply taking a fraction of the biomass by:

$$C = 0.475 \times B$$ ....Eq 10

Where, C is carbon content by mass, and B is oven-dry biomass.

4.9 Indigenous and exotic trees carbon storage

Relationship among the twenty tree species collected from Yala basin was explored by cluster analysis based on Euclidean distance under taken using an un-weighted pair group method with arithmetic averaging. The species were divided into indigenous and exotic (Table 18), proximity matrix showed four major clusters (Figure 16); the clustering was based on species carbon and their distances shown in Table 18.
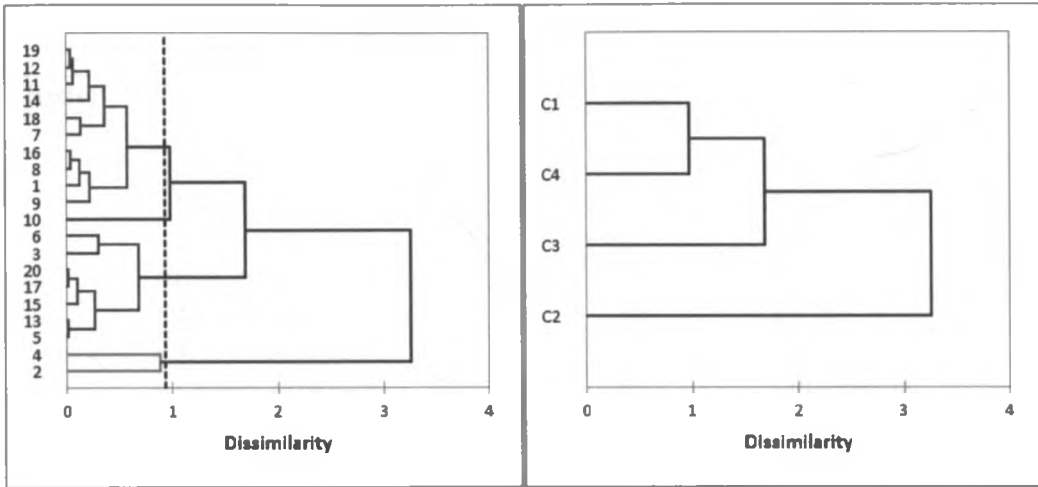
Figure 16: Dendogram based on Euclidean distance for 20 tree species.

The cluster numbers in the dendogram corresponds to species as given in the key of table 18 and their corresponding types. However, the cluster distances are given in Table 17.

Table 17: Distances between four clusters among 20 species from Yala basin.

	C1(Indigenous)	C2 (Indigenous)	C3 (Exotic)
C1 (Indigenous)			
C2 (Indigenous)	3.210		
C3 (Exotic)	1.040	2.170	
C4 (Exotic)	0.940	4.150	1.980

The mean carbon values for indigenous cluster 1 and 2 were 48.23% and 45.02% respectively. While the exotic clusters 3 and 4 had carbon values of 49.17% and 47.19% respectively.

Table 18: Classification of species types and corresponding cluster number.

Cluster	Species	Key	Type of species
1	*Acacia mearnsii*	1	Exotic
	Eucalyptus grandis	7	Exotic
	Eucalyptus saligna	8	Exotic
	Ficus spp	9	Indigenous
	Harungana madagascariensis	11	Indigenous
	Jacaranda mimosifolia	12	Exotic
	Markhamia lutea	14	Indigenous
	Prunus africana	16	Indigenous
	Syzygium cordatum	18	Indigenous
	Syzygium cuminii	19	Exotic
2	*Bridelia micrantha*	2	Indigenous
	Croton macrostachyus	4	Indigenous
3	*Combretum molle*	3	Exotic
	Cupressus lusitanica	5	Exotic
	Eucalyptus camaldulensis	6	Exotic
	Mangifera indica	13	Exotic
	Persea americana	15	Exotic
	Spathodea campanulata	17	Indigenous
	Trilepisium madagascariensis	20	Indigenous
4	*Grevillea robusta*	10	Exotic

Key: Numbers match the corresponding species name in Figure 16

The results in Figure 16 showed no clear pattern among the indigenous and exotic species in terms of their carbon distribution, this could be due to the fact that trees have different characteristics in terms of metabolism and growth resulting in various C-containing compounds (Kozlowski, 1992), the variations in C are influenced by site conditions, tree age and management practice (Elias and Potvin, 2003).

Cluster 2 had only indigenous species while cluster 4 had only exotic, the number of *G. robusta* sampled was one, thus complicating explanation for cluster 4. A minimum of five trees are recommended by Williamson and Wiemann (2010) while sampling tree species, this indicates that the number of trees required in a given ecosystem depends on the variability within the species.

4.10 Spectral measurements

4.10.1 Spectral signatures

Cored samples exhibited distinct spectral signatures for both the NIR and MIR spectral regions, differences between the bands of individuals wood samples in the NIR and MIR spectral regions are difficult to distinguish, showing only as broad humps as shown in Figures 17 and 20. These are spectral signatures from the three blocks (Middle Yala, Lower Yala and Upper Yala). Near Infrared spectral acquisition in the range of 4,000 cm^{-1} to 8,000 cm^{-1} (Figure 17) and 600 cm^{-1} to 4,000 cm^{-1}(Figure 18) for Mid-Infrared regions.
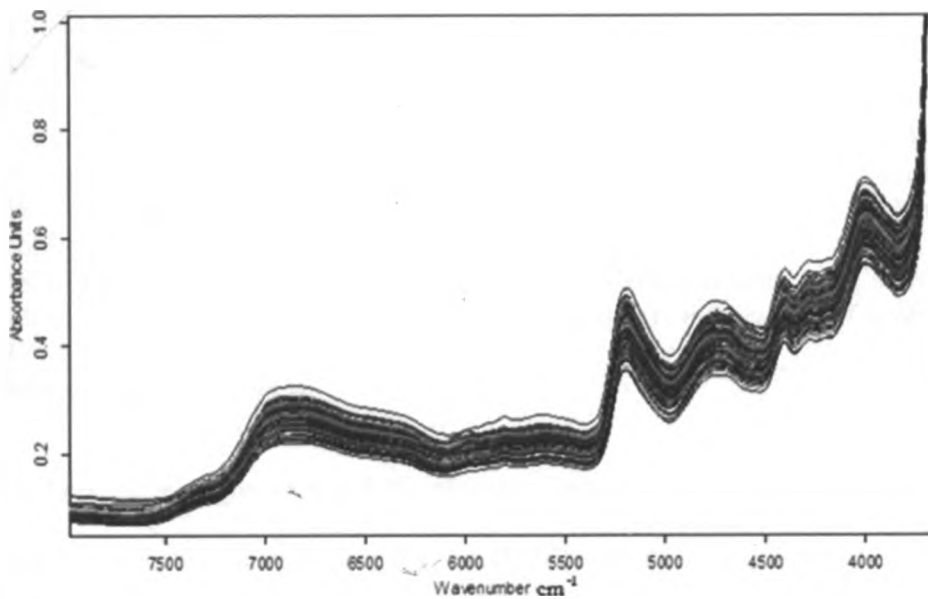
Figure 17: Spectral signatures for Near Infrared spectra region.

Major absorption bands for core samples were found in the wavelength region at 6940-6900, 5700-5630 and 5650-5600, 4850-4780, 4400-4380 and 4220-4180 cm^{-1} in the NIR

spectral region. Bonds with more s character absorb at high frequency, Sp^3 (C-H) just

below 3000 cm^{-1} to the right, SP^2 (C-H) just above 3000 cm^{-1} to the left and SP (C-H) at

3300 cm^{-1}. O-H stretch of carboxylic acid (COOH) absorbs broadly due to strong

hydrogen bonding at $2500cm^{-1}$. Also notable peak around 5650-5600 cm^{-1} could be as a

possible result of $-CH_3$ stretch in first harmonic region and various functional groups

present in different tree species of wood samples, specific absorption bands are as shown

in table 19.

Table 19: Specific absorption bands in near Infrared spectra of wood cores.

Wavenumber (cm^{-1})	Chemical Group	Characteristic vibration	Spectral region
12000-9000		Noisy region	3rd harmonic
9350-9220	-CH and C-C	Stretch	Combination
8850-8770	Aromatic		2nd harmonic
8700-8580;8840-8370 and 8400-8330	-CH3	Stretch	2nd harmonic
7170-7020	-OH	Bend	1st harmonic
7090-7040 and 6940-6900	-CH and CH	Stretch and bend	Combination
5950-5920	Aromatic		1st harmonic
5850-5870;5700-5630 and 5650-5600	-CH3	Stretch	1st harmonic
4850-4780	-OH	Stretch and bend	Combination
4400-4380	CH-	Stretch and bend	Combination
4220-4180	-OH	Stretch	2nd harmonic

Source: Banwell (1983)

In the spectral signatures in MIR region (Figure 18), dominant absorption features were

observed in the following region: 3400, 1750-1600, 2970, 2250, 2220, 1750-1600 and

1200-1000 cm^{-1} suggesting the following functional groups; $-NH_2$, $-CH_3$, $-C{\equiv}N$, $-C{\equiv}C$,

$>C=O$ and from 1200-1000 cm^{-1}; -C-C-, -C-N and -C-O-.
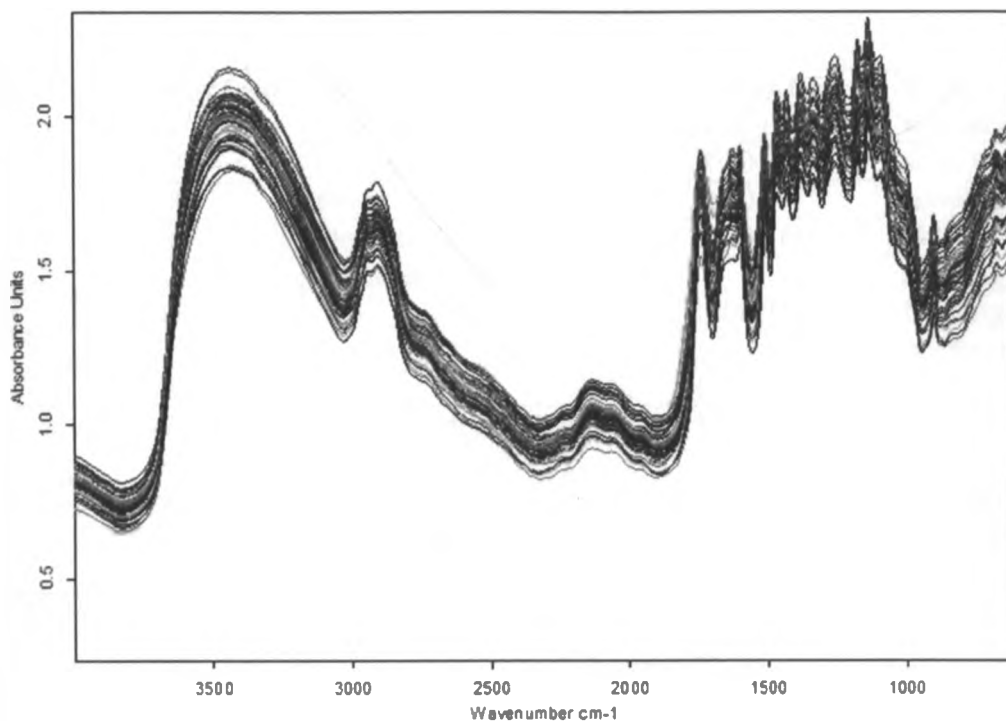
Figure 18: Full range spectral signatures for mid-Infrared spectra region.

The distinct fingerprint region of Mid-Infrared from 1200-600 cm^{-1} is hard to resolve but is useful since different species have different compounds with distinct fingerprint signatures. Table 20 has characteristic stretching frequencies for some of molecular groups around MIR region. The finger print region shows both the skeletal vibrations-involving all atoms and the characteristic group vibrations which only involves small portion of the molecule, with the remainder being more or less stationary. Skeletal frequencies are in the range of 1400-700 cm^{-1} and arise from linear or branched chain structures (Banwell, 1983). The high peak around 1350 cm^{-1} is due to C–H and O–H bending vibrations (Banwell, 1983).

Table 20: Characteristic stretching frequencies in MIR region

Group	Appox.freq (cm^{-1})	Type of vibration	Group	Appox.freq (cm^{-1})	Type of vibration
-OH	3600	bending in-plane	>C=C<	1650	scissoring, or bending in-plane
-NH$_2$	3400		>C=N-	1600	
≡CH	3300	Deformation and stretching	>C=O	1750-1600	
⬡	3060		C-C≡ C-N< C-O-	1200-1000	twisting, or bending out-of-plane
=CH$_2$	3030		>C=S	1100	
-CH$_3$	2970,2870	Asymmetrical stretching	>C-F	1050	
-CH$_2$-	2850	symmetrical stretching	C-Cl	725	Rocking, or bending in-plane
-SH	2580	stretching	C-Br	650	scissoring, or bending
-C≡N	2250		C-I	550	
-C≡C	2220			1350-1150 cm-1	

Source: Banwell (1983)

4.10.2 Spectral pre-processing

First derivatives spectral pre-treatment technique (Figure 19 andFigure **20**) gave the data for chemometric modelling by subtracting each variable (point) in a sample from its immediate neighbouring variable (point) thus, removing the same signal between the two variables leaving only the part of the signal which is different.

The spectral range extending from 9,000 to 12,500 cm^{-1} in NIR had high noise level corresponding to the third harmonic region. It was excluded for calibration since it is characterized by low absorption and has poor information quality (Hein *et al.*, 2009).
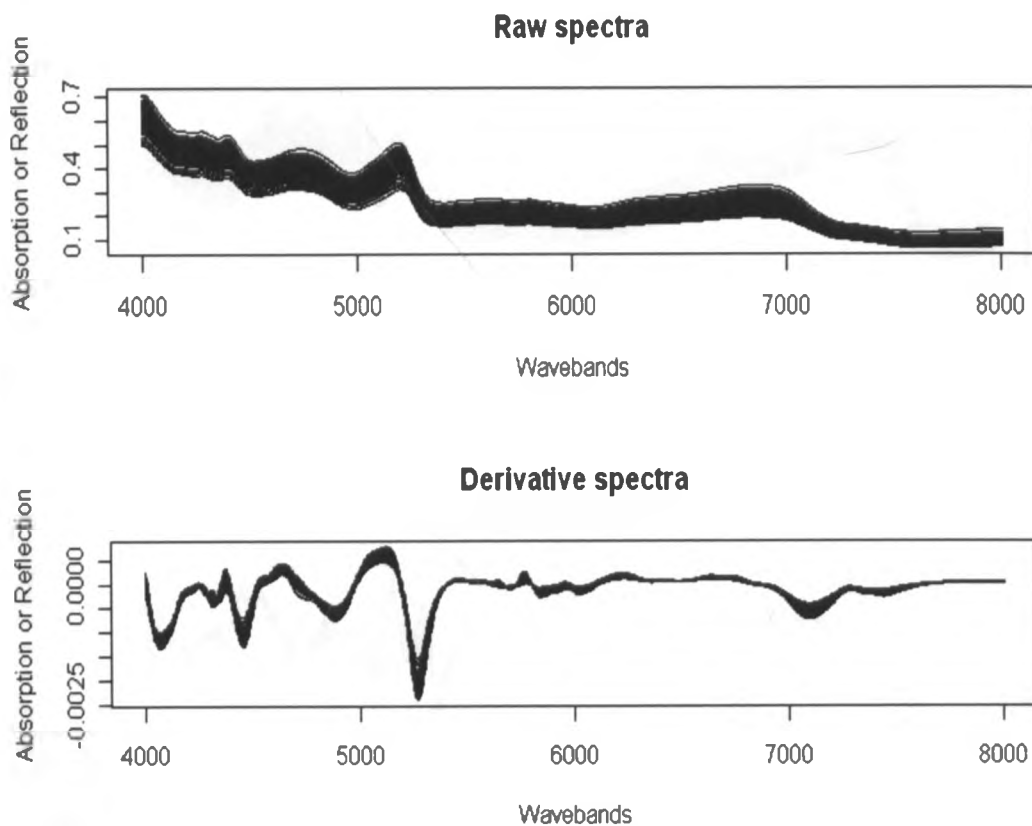
Figure 19: Reduced raw and first derivative of NIR spectra.

Hein *et al.*, (2009) reported the application of spectral filter, exclusion of outliers and selection of variables wavelengths as a way of improving statistics associated with models. Similarly Jones *et al.*, (2006) also reported improvement while studying basic density of 120 samples of *Pinus taeda.* These findings demonstrated that application of spectral data pre-treatment of the first derivative reduced the standard error of prediction (SEP) but increased ratio performance deviation (RPD).

Raw spectra

Derivative spectra
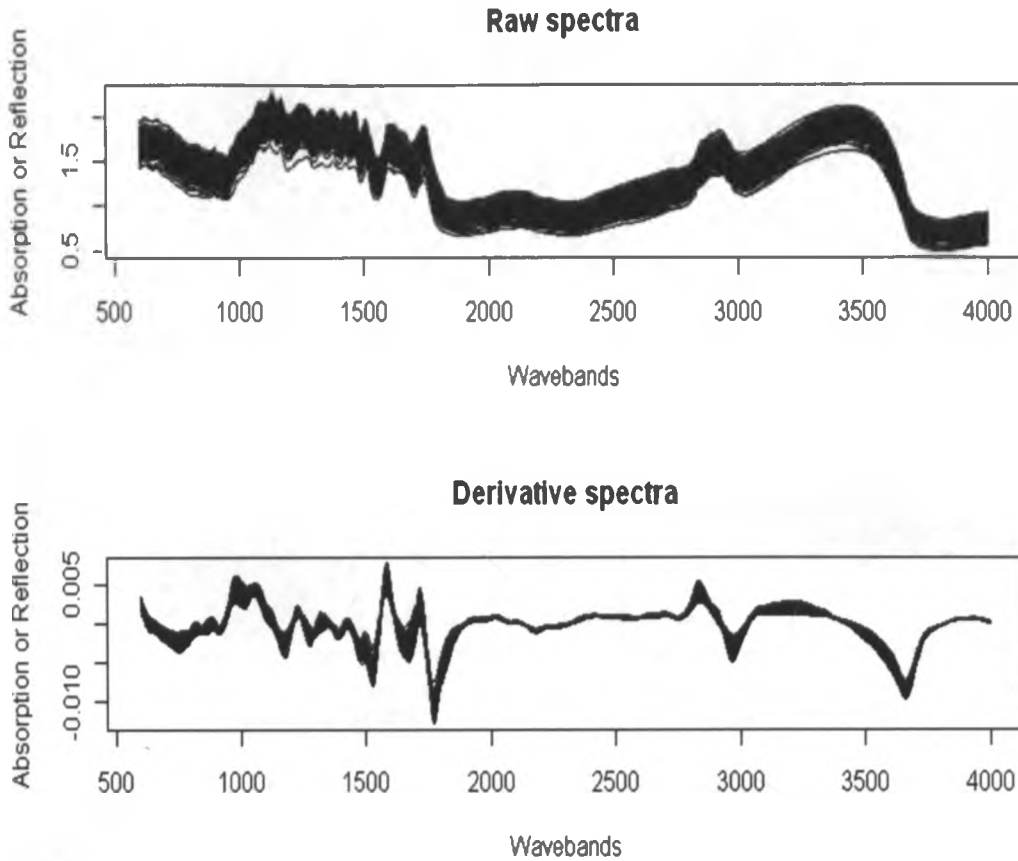
Figure 20: Raw and first derivative of Mid-Infrared spectra.

4.10.3 Selected samples

The selected representative samples (Figure 21) were based on recorded NIR and MIR spectral diversity using the Kennard-Stone algorithm and calculated from principal component scores (PCs). The PCs approximates the original data to desired degree of accuracy (Cozzolino *et al.,* 2009), transforming a set of correlated variables into a smaller number of uncorrelated variables called latent variables. Other different calibration sets followed the same principle. The pictorial representation (Figure 21) helps to visualise whether the selected samples are really representative.

68
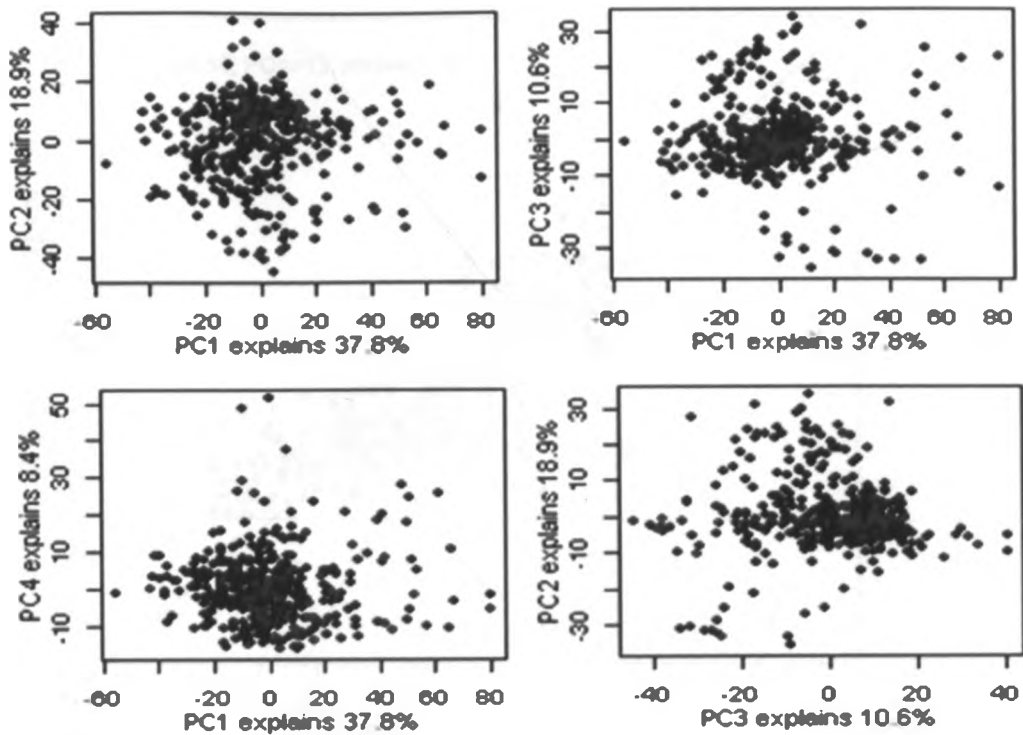
Figure 21: Selection based on 10% with red indicating selected samples

4.11 PLS Calibration

4.11.1 Developing a calibrations using all samples set

In this approach all the samples are used as the calibration set, expecting best calibration thus, giving the best indication of the potential of mid-IR or NIR as useful tool for determining physical and chemical composition (Bellon-Maurel and McBratney, 2011). The calibration performance was low (Table 21, Figures 22 and 23) with low R^2 values both for MIR and NIR, making it virtually impossible for the calibration to determine accurately the composition of new samples from their spectra alone.
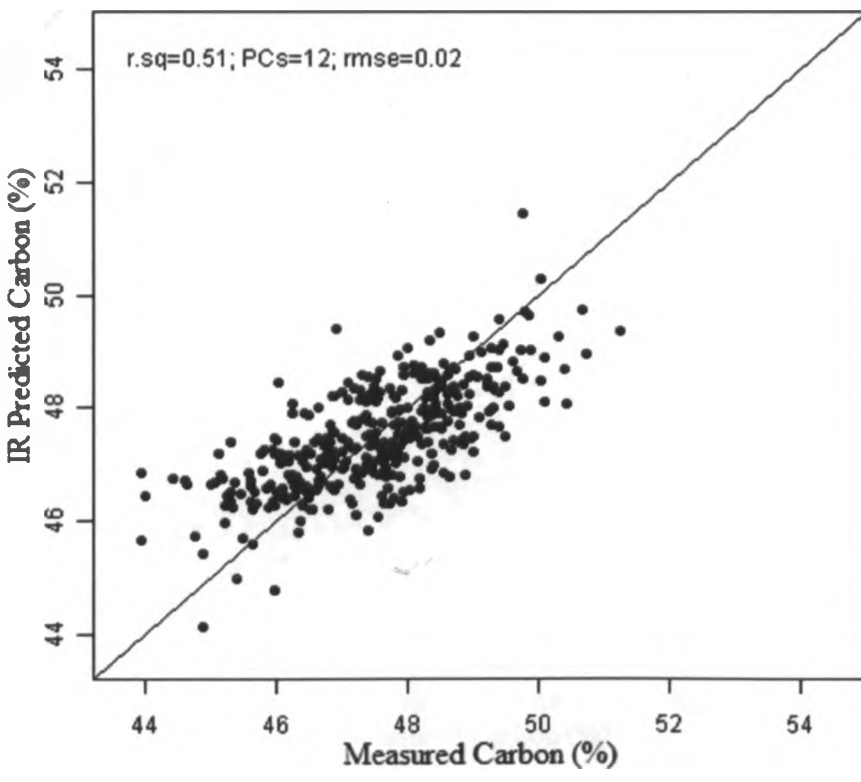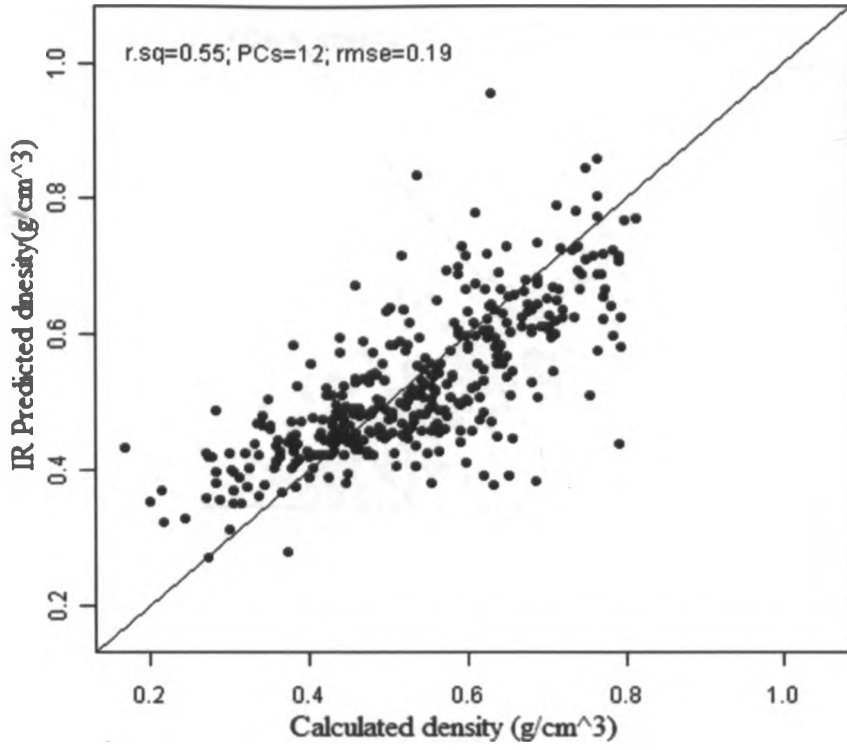
Figure 22: NIR PLS Calibration models for density and carbon
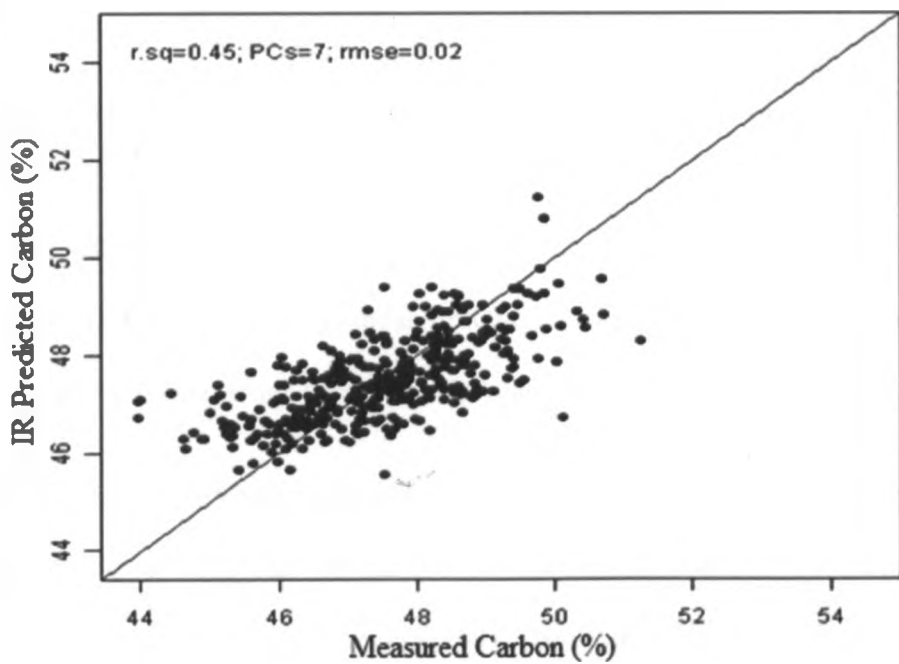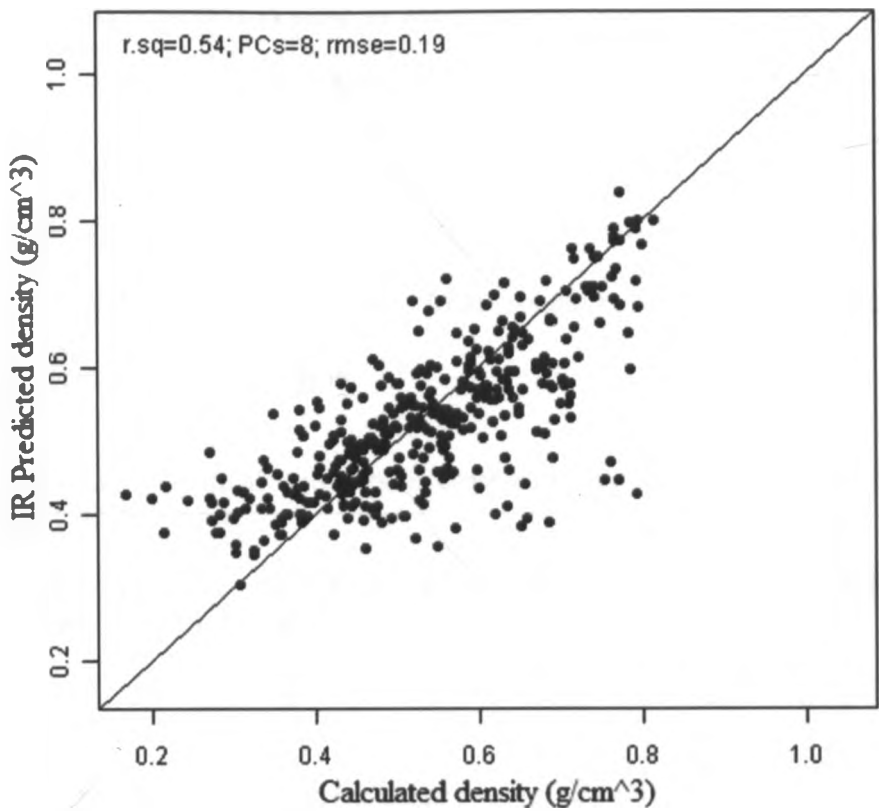
Figure 23: MIR PLS Calibration models for density and carbon

The data presented in table 21 show that the Nir-IR calibrations in terms of R^2 for WD was fairer at (R^2=0.55), while the rest were poor with R^2<0.50. Mid-IR calibrations were not good either with nitrogen (R^2=0.51) and the other properties having R^2<0.50. With only a few exceptions, calibrations based on Nir-IR spectra were better (larger R^2 and smaller RMSECV) than their MIR counterparts even after removing wavelengths associated with CO_2 region.

Table 21: Statistical summary of cross-validated calibration results using all samples as the calibration set

IR range	n	Property	PCs	R^2	Bias	RMSECV
NIR	373	WD	12	0.55	-0.03	0.17
	375	C	12	0.51	-3.48	12.59
	389	N	9	0.48	-0.04	0.09
	381	Cg	6	0.49	0.02	0.11
	380	Ng	9	0.38	-6E-05	6E-04
MIR	373	WD	6	0.42	-0.03	0.18
	375	C	8	0.49	-3.37	12.92
	389	N	9	0.51	-0.04	0.09
	381	Cg	6	0.43	0.02	0.11
	380	Ng	9	0.42	-4E-05	6E-04

Key: WD = wood density (gcm^{-3}), C =carbon (%), N = Nitrogen, Cg =carbon (gcm^{-3}), n=total number of samples after removal of outliers

The calculated principle components (PCs) were affected by various wave-lengths attributable to various chemical structures and compounds (Chodak et al., 2007); PCs reduced the data points describing the manipulated NIR /MIR spectra.

For wood density prediction using MIR spectra (90% Calibset), PC1 was dominated by absorption at 1890 and 700 cm^{-1}, which may be attributed to COOH groups (Figure 24). PC2 was affected mainly by absorption between 3,500 and 2,500 cm^{-1} (attributable to CH_3 groups) and PC3 by absorption at 3,670, 3,300, and 2,350 nm (attribued to CH_2 and CH_3 groups).
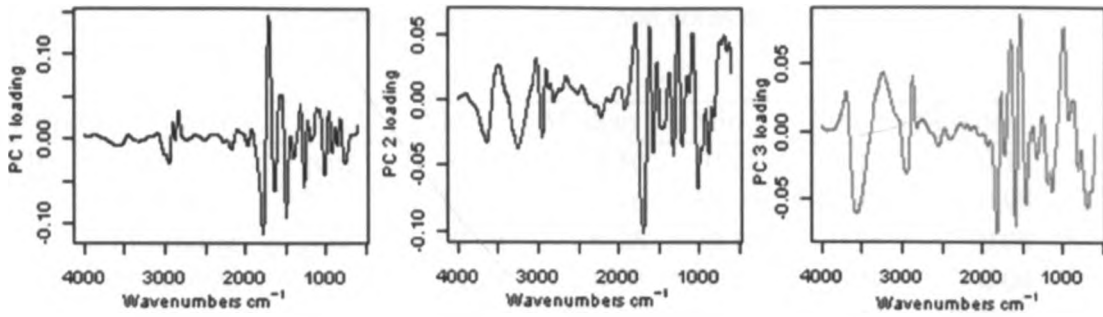
Figure 24: Plot of factor loading values for the PCs for MIR spectra

From the means of these three methods (Table 22), predicted mean wood density values from NIR and MIR was 0.527 gcm^{-3} and 0.528 gcm^{-3} while the calculated density was 0.59 gcm^{-3}. Mean carbon predicted was 47.58% (NIR), 47.59% (MIR) and laboratory measured mean carbon value was 47.61%. Mean IR predicted nitrogen was 0.24% (NIR) and 0.24% for MIR, while laboratory determined value was 0.28%. Predicted Carbon (gcm^{-3}) from NIR and MIR spectra had the same mean values of 0.28 gcm^{-3}, but low mean laboratory values of 0.24 gcm^{-3}. Mean nitrogen in (gcm^{-3}) was the same for both the IR and laboratory measured values (0.0014 gcm^{-3}). The standard deviation of these properties were small given that the predictions were from different ranges of wavelengths (NIR and MIR) compared to the values obtained by laboratory measurement.

Table 22: Chemical and physical properties of wood cores determined using the three different methods.

Method	Property	Unit	Mean	Median	Min	Max	Std.dev
NIR	Density	gcm^{-3}	0.53	0.50	0.25	0.95	0.11
	Carbon	%	47.58	47.46	44.14	51.45	0.98
	Carbong	gcm^{-3}	0.28	0.26	0.14	0.56	0.06
	Nitrogen	%	0.24	0.23	0.18	0.47	0.04
	Nitrogeng	gcm^{-3}	0.0014	0.0013	0.0007	0.0034	0.0004
MIR	Density	gcm^{-3}	0.53	0.52	0.32	0.86	0.11
	Carbon	%	47.59	47.44	45.56	51.24	1.01
	Carbong	gcm^{-3}	0.28	0.27	0.15	0.45	0.06
	Nitrogen	%	0.24	0.23	0.18	0.38	0.04
	Nitrogeng	gcm^{-3}	0.0014	0.0013	0.0005	0.0038	0.0004
MD	Density	gcm^{-3}	0.59	0.58	0.20	0.95	0.16
	Carbon	%	47.61	47.60	39.62	52.14	1.52
	Carbong	gcm^{-3}	0.24	0.23	0.02	0.49	0.06
	Nitrogen	%	0.28	0.28	0.09	0.48	0.08
	Nitrogeng	gcm^{-3}	0.0014	0.0014	0.0001	0.0036	0.0005

Key: CD = Calculated density, MD =Measured density

Subjecting the mean values to Pearson correlation, all properties of the variables had positive correlation coefficients with P values greater than 0.050, implying that there was no significant relationship between the means.

4.11.2 Prediction of species properties from whole samples model

The output in Figure 25 shows the results of a fitted linear model describing the relationship between IR (MIR/NIR) predicted values against calculated/laboratory measured values of 20 species using mean values from whole samples prediction model.
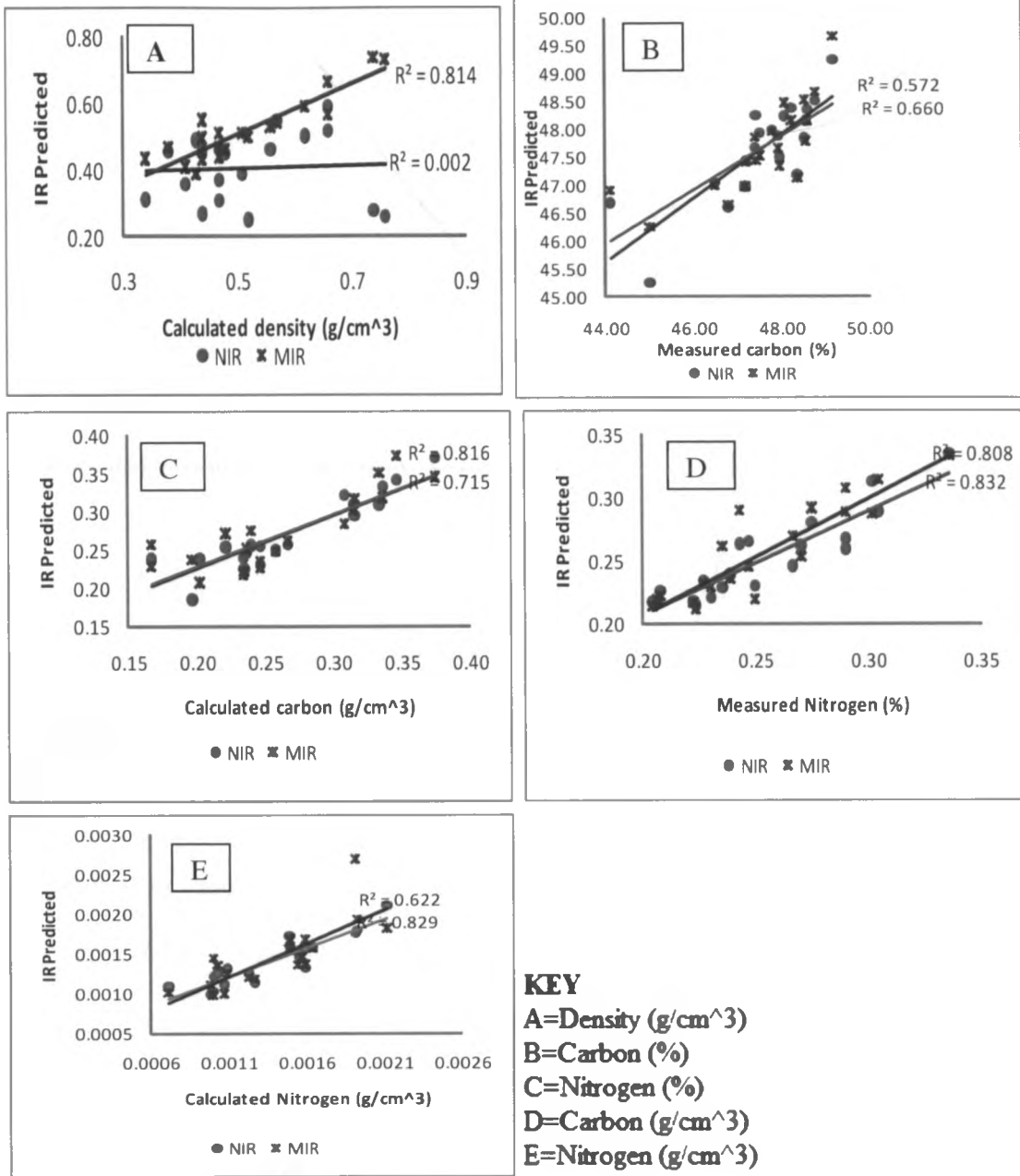
Figure 25: A model between IR predicted and measured values (all samples)

These linear models shows that when the values averaged to the species level the prediction is much better than the individual core models, an indication that large within species variations exist that cannot be predicted using IR. But in general all other properties were well predicted using NIR with both models showing statistically

significant relationship. The nitrogen content both calculated (gcm^{-3}) and measured (%) had good correlation with NIR predicted values with R^2 of 0.83. While MIR gave R^2 of 0.62 and 0.80 respectively. For NIR, carbon both calculated (gcm^{-3}) and measured (%) gave R^2 value of 0.66 and 0.82 respectively, and 0.57 and 0.72 respectively for MIR. In NIR the predicted values gave a correlation coefficient greater than 0.080, indicating strong relationship.

4.11.3 Calibration and validation using 50/50 split

Table 23 lists performance details of the analysis of PLS models for wood properties. For carbon, the calibration model performed better than the initial model developed using the entire samples, with the R^2 value improving from 0.51 to 0.75 for calibration, and 0.31 for validation in NIR region (Figure 27).

The R-Square validation set explains 30.68% of the variability in predicted values, while the correlation coefficient equals 0.55, indicating a moderately strong relationship between the variables. While for MIR R^2 value improved from 0.45 to 0.53 for calibration, and 0.40 for validation (Figure 26). The validation model explains 40.43% of the variability in predicted set.

The correlation coefficient equals 0.64 indicates a moderately strong relationship between the variables, other properties were poorer with $R^2 < 50$ in calibration sets. For density, nitrogen model had similar performance, while the SECV showed a small increase in the 50/50 model.
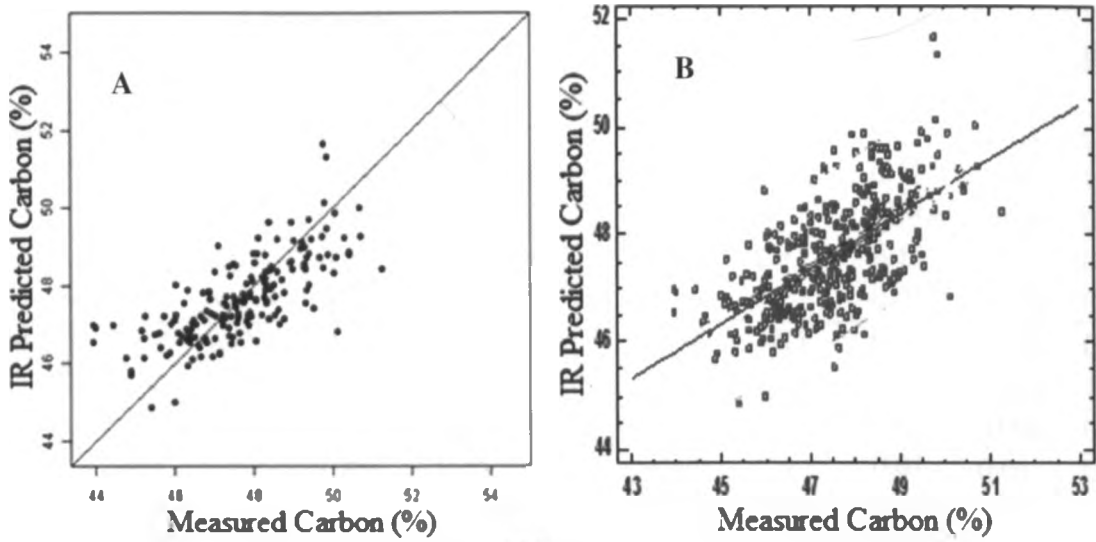
Figure 26: MIR PLS models for carbon (A) Calibration and (B) validation.
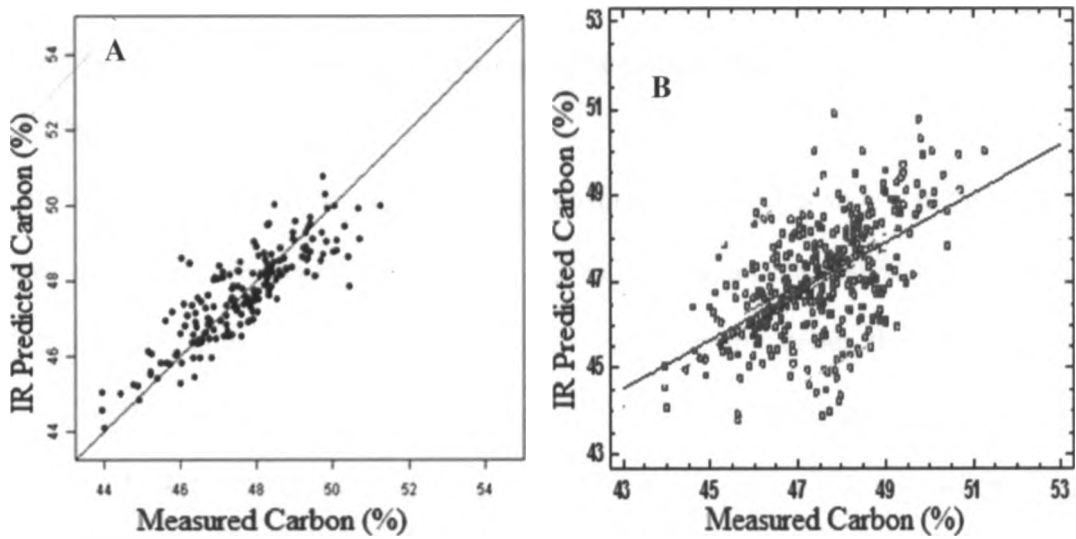
Figure 27: NIR PLS models for carbon (A) Calibration and (B) validation.

Table 23: Cross-validated calibration and Independent validation results for NIR and MIR region of spectra based on 50/50 split.

	Calibration					Validation				
IR range	n	Property	R^2	RMSECV	PCs	n	Property	R^2	Bias	RMSEP
NIR	187	WD	0.24	0.21	2	186	WD	0.19	-0.03	0.18
	186	C	0.75	0.02	12	187	C	0.31	-3.07	12.71
	195	N	0.07	0.22	2	194	N	9E-06	-0.04	0.08
	191	Cg	0.33	0.23	3	190	Cg	0.18	0.01	0.10
	190	Ng	0.11	0.33	2	190	Ng	0.05	0.000	0.001
MIR	187	WD	0.39	0.19	3	186	WD	0.31	-0.04	0.19
	186	C	0.53	0.02	7	187	C	0.40	-3.50	12.95
	195	N	0.32	0.2	3	194	N	0.03	-0.04	0.08
	191	Cg	0.39	0.23	3	190	Cg	0.01	0.01	0.11
	190	Ng	0.31	0.3	3	190	Ng	0.28	0.000	0.001

Key: WD = wood density (gcm^{-3}), C =carbon (%), N = Nitrogen, Cg =carbon (gcm^{-3}), n=total number of samples

4. 11.4 Prediction of species properties using 50/50 split model

Statistical summary of predictions developed using 50/50 split is shown in table 24; the mean values were regressed against measured values (Figure 28). At 95.0% confidence level, the predictions developed using MIR was generally better than NIR; density R^2=0.51(MIR) and R^2=0.46 (NIR), carbon (%) R^2=0.60 (MIR) and R^2=0.48 (NIR), nitrogen (%) R^2=0.66 (MIR) and R^2=0.02 (NIR), carbon (gcm^{-3}) and nitrogen (gcm^{-3}) R^2<0.50 for both MIR and NIR.
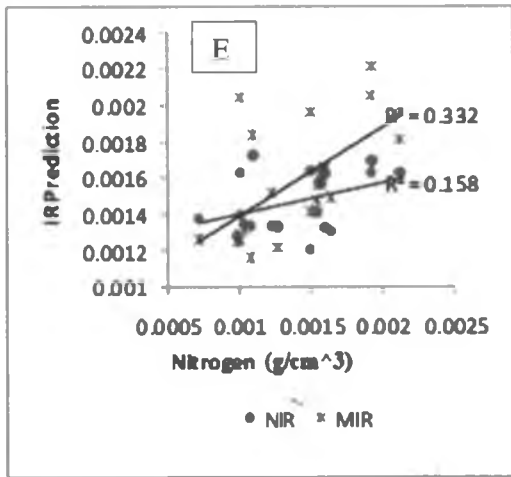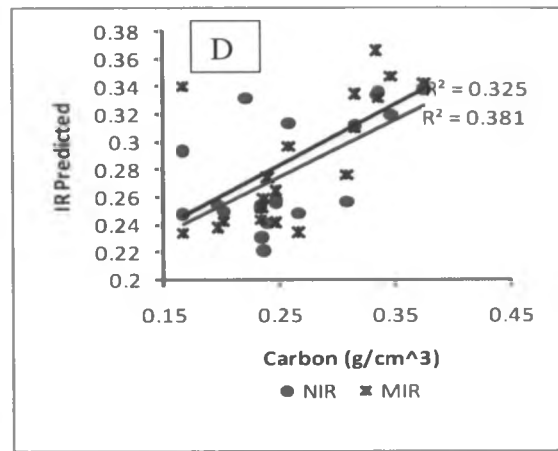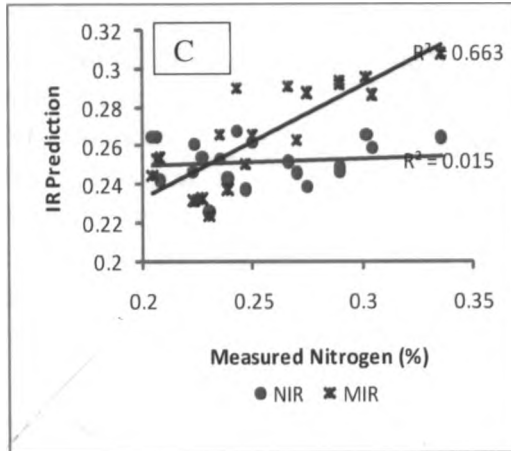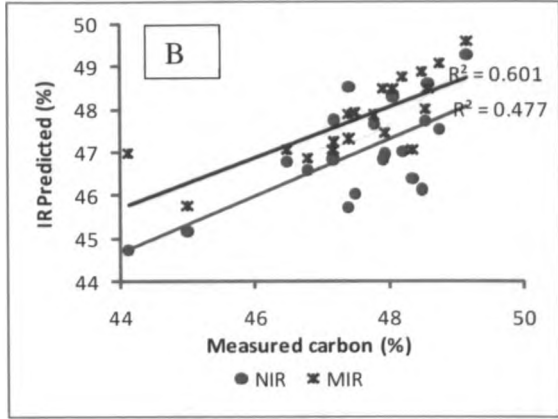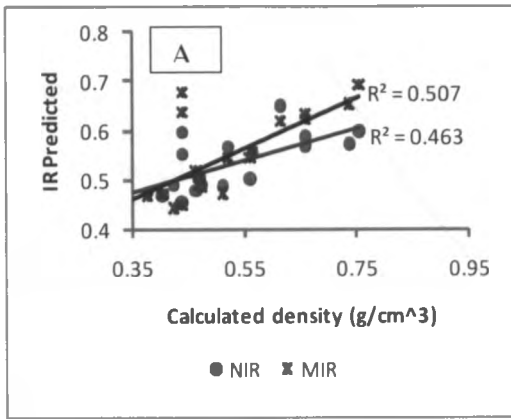
KEY
A=Density (g/cm^3)
B=Carbon (%)
C=Nitrogen (%)
D=Carbon (g/cm^3)
E=Nitrogen (g/cm^3)

Figure 28: A 50/50 split model between IR predicted and measured values.

Table 24: Summary statistics of predicted values using 50/50 split mode

Property	Mean	Min	Max	S.D	C.V (%)
Density (gcm^{-3})	0.52	0.34	0.76	0.12	0.23
MIR Predicted	0.55	0.44	0.69	0.08	0.15
NIR Predicted	0.53	0.45	0.65	0.05	0.10
Carbon (%)	47.56	44.13	49.17	1.24	0.03
MIR Predicted	47.80	45.74	49.58	0.93	0.02
NIR Predicted	47.02	44.71	49.26	1.17	0.02
Nitrogen (%)	0.25	0.20	0.34	0.04	0.15
MIR Predicted	0.26	0.22	0.31	0.03	0.10
NIR Predicted	0.25	0.23	0.27	0.01	0.05
Carbon (gcm^{-3})	0.26	0.17	0.38	0.06	0.23
MIR Predicted	0.29	0.23	0.37	0.05	0.16
NIR Predicted	0.28	0.22	0.34	0.04	0.14
Nitrogen (gcm^{-3})	0.001	0.001	0.002	0.000	0.27
MIR Predicted	0.002	0.001	0.002	0.000	0.20
NIR Predicted	0.001	0.001	0.002	0.000	0.11

Key: Min=Minimum, Max=maximum, S.D=Standard deviation, C.V=Coefficient of variation

The properties of the variables had positive correlation coefficients with $P > 0.05$, except in the density estimation where $P < 0.05$.

4.11.5 Varying percentages of Calibration set

Table 25 and 27 shows results for calibration sets of 10%, 20%, 30%, 50%, 60%, 70%, 80% and 90% for the properties in both NIR and MIR region. While tables 26 and 28 shows the independent validations sets. Coefficient of determination (R^2), bias and root mean square error of prediction (RMSEP) shows the predictive performance for cross-validated calibrations results and independent validations.

Table 25: NIR Cross-validated calibration results.

Calib set	Property	R^2	PCs	RM SECV	Calib set	Property	R^2	PCs	RM SECV	Calib set	Property	R^2	PCs	RM SECV
10%	WD	0.27	1	0.19	40%	WD	0.24	2	0.21	70%	WD	0.33	4	0.2
10%	C	0.42	2	0.02	40%	C	0.75	12	0.02	70%	C	0.76	15	0.01
10%	N	0.35	2	0.19	40%	N	0.13	2	0.21	70%	N	0.03	1	0.22
10%	Cg	0.13	1,	0.19	40%	Cg	0.21	2	0.24	70%	Cg	0.48	10	0.2
10%	Ng	0.03	1	0.3	40%	Ng	0.03	1	0.33	70%	Ng	0.39	10	0.28
20%	WD	0.5	3	0.17	50%	WD	0.24	2	0.21	80%	WD	0.52	12	0.17
20%	C	0.53	2	0.02	50%	C	0.75	12	0.02	80%	C	0.37	4	0.02
20%	N	0.45	3	0.18	50%	N	0.07	2	0.22	80%	N	0.31	7	0.21
20%	Cg	0.36	3	0.2	50%	Cg	0.33	3	0.23	80%	Cg	0.5	11	0.2
20%	Ng	0.02	1	0.31	50%	Ng	0.11	2	0.33	80%	Ng	0.42	10	0.32
30%	WD	0.33	3	0.17	60%	WD	0.53	11	0.16	90%	WD	0.53	12	0.19
30%	C	0.64	6	0.01	60%	C	0.76	14	0.02	90%	C	0.5	11	0.02
30%	N	0.04	1	0.22	60%	N	0.03	1	0.22	90%	N	0.5	11	0.19
30%	Cg	0.32	3	0.19	60%	Cg	0.27	2	0.25	90%	Cg	0.49	11	0.21
30%	Ng	0.03	1	0.32	60%	Ng	0.09	2	0.35	90%	Ng	0.42	12	0.31

Key: WD = wood density (gcm^{-3}), C =carbon (%), N = Nitrogen, Cg =carbon (gcm^{-3}), Ng = Nitrogen (gcm^{-3})

Table 26: NIR Independent validation results.

Calib set	Property	R^2	Bias	RMSEP	Calib set	Property	R^2	Bias	RMSEP	Calib set	Property	R^2	Bias	RMSEP
10%	WD	0.46	-0.02	0.18	40%	WD	0.43	-0.02	0.18	70%	WD	0.30	-0.07	0.18
10%	C	0.48	-3.47	12.63	40%	C	0.30	-2.94	12.71	70%	C	0.10	-4.29	12.47
10%	N	0.01	-0.04	0.09	40%	N	0.00	-0.03	0.08	70%	N	0.01	-0.07	0.08
10%	Cg	2E-05	0.02	0.11	40%	Cg	0.03	0.02	0.10	70%	Cg	0.10	0.01	0.10
10%	Ng	0.36	-6E-05	6E-04	40%	Ng	0.10	-0.02	0.18	70%	Ng	0.001	0.000	0.001
20%	WD	0.48	-0.04	0.18	50%	WD	0.19	-0.03	0.18	80%	WD	0.14	-0.09	0.20
20%	C	0.34	-3.32	12.58	50%	C	0.31	-3.07	12.71	80%	C	4E-05	-4.29	12.34
20%	N	0.001	-0.05	0.09	50%	N	9E-06	-0.04	0.08	80%	N	0.01	-0.07	0.08
20%	Cg	0.01	0.03	0.10	50%	Cg	0.18	0.01	0.10	80%	Cg	0.22	0.01	0.11
20%	Ng	0.34	-8E-05	0.001	50%	Ng	0.05	0.000	0.001	80%	Ng	0.00	0.000	0.001
30%	WD	0.36	-0.04	0.18	60%	WD	0.18	-0.05	0.19	90%	WD	0.014	-0.08	0.19
30%	C	0.31	-2.89	12.74	60%	C	0.23	-3.61	12.59	90%	C	0.10	-3.67	12.47
30%	N	0.00	-0.05	0.09	60%	N	0.00	-0.05	0.08	90%	N	0.01	-0.07	0.08
30%	Cg	0.004	0.03	0.10	60%	Cg	0.20	0.00	0.10	90%	Cg	0.01	0.04	0.10
30%	Ng	0.34	0.000	0.001	60%	Ng	1E-05	0.000	0.001	90%	Ng	0.01	0.000	0.001

Key: WD = wood density (gcm^{-3}), C = carbon (%), N = Nitrogen, Cg = carbon (gcm^{-3}), Ng = Nitrogen (gcm^{-3})

Table 27: MIR Cross-validated calibration results.

Calib set	Property	R^2	PCs	RM SECV	Calib set	Property	R^2	PCs	RM SECV	Calib set	Property	R^2	PCs	RM SECV
10%	WD	0.50	2	0.14	40%	WD	0.49	6	0.16	70%	WD	0.5	8	0.16
10%	C	0.76	5	0.01	40%	C	0.62	7	0.02	70%	C	0.57	8	0.02
10%	N	0.65	4	0.15	40%	N	0.35	3	0.2	70%	N	0.36	5	0.19
10%	Cg	0.41	2	0.15	40%	Cg	0.42	7	0.19	70%	Cg	0.47	8	0.2
10%	Ng	0.40	2	0.26	40%	Ng	0.26	3	0.29	70%	Ng	0.44	8	0.26
20%	WD	0.50	1	0.22	50%	WD	0.39	3	0.19	80%	WD	0.47	7	0.17
20%	C	0.71	6	0.01	50%	C	0.53	7	0.02	80%	C	0.53	9	0.02
20%	N	0.70	5	0.13	50%	N	0.32	3	0.2	80%	N	0.4	7	0.2
20%	Cg	0.39	3	0.19	50%	Cg	0.39	3	0.23	80%	Cg	0.47	6	0.21
20%	Ng	0.14	1	0.22	50%	Ng	0.31	3	0.3	80%	Ng	0.48	10	0.29
30%	WD	0.49	3	0.15	60%	WD	0.41	2	0.2	90%	WD	0.5	8	0.2
30%	C	0.58	3	0.02	60%	C	0.57	8	0.02	90%	C	0.46	7	0.02
30%	N	0.35	3	0.19	60%	N	0.35	5	0.19	90%	N	0.47	7	0.19
30%	Cg	0.36	3	0.18	60%	Cg	0.50	7	0.2	90%	Cg	0.37	3	0.24
30%	Ng	0.32	3	0.28	60%	Ng	0.45	8	0.27	90%	Ng	0.41	8	0.31

Key: WD = wood density (gcm^{-3}), C =carbon (%), N = Nitrogen, Cg =carbon (gcm^{-3}), Ng = Nitrogen (gcm^{-3})

Table 28: MIR Independent validation results.

Calib set	Property	R^2	Bias	RM SEP	Calib set	Property	R^2	Bias	RM SEP	Calib set	Property	R^2	Bias	RM SEP
10%	WD	0.47	-0.03	0.015	40%	WD	0.39	-0.05	0.19	70%	WD	0.33	-0.09	0.18
10%	C	0.45	-3.37	12.99	40%	C	0.41	-3.32	13.03	70%	C	0.00	-4.42	12.70
10%	N	4E-05	-0.05	0.09	40%	N	0.02	-0.05	0.09	70%	N	0.03	-0.08	0.08
10%	Cg	0.001	0.02	0.11	40%	Cg	0.00	0.01	0.11	70%	Cg	0.1	0.02	0.11
10%	Ng	0.33	0.000	0.001	40%	Ng	0.28	0.000	0.001	70%	Ng	0.15	0.000	0.001
20%	WD	0.50	-0.05	0.18	50%	WD	0.31	-0.04	0.19	80%	WD	0.21	-0.12	0.19
20%	C	0.38	-3.29	12.80	50%	C	0.40	-3.50	12.95	80%	C	0.01	-4.47	12.88
20%	N	0.006	-0.06	0.10	50%	N	0.03	-0.04	0.08	80%	N	0.10	-0.09	0.09
20%	Cg	0.13	0.02	0.11	50%	Cg	0.01	0.01	0.11	80%	Cg	0.00	0.04	0.12
20%	Ng	0.31	0.000	0.001	50%	Ng	0.28	0.000	0.001	80%	Ng	0.16	-0.12	0.19
30%	WD	0.50	-0.05	0.18	60%	WD	0.27	-0.08	0.20	90%	WD	0.26	-0.07	0.18
30%	C	0.42	-3.26	12.99	60%	C	0.08	-4.07	12.68	90%	C	0.00	-4.14	12.86
30%	N	0.01	-0.33	0.09	60%	N	0.00	-0.07	0.09	90%	N	0.04	-0.08	0.09
30%	Cg	0.004	0.02	0.11	60%	Cg	0.03	0.01	0.11	90%	Cg	0.02	0.04	0.12
30%	Ng	0.31	0.000	0.001	60%	Ng	0.17	0.000	0.001	90%	Ng	0.05	-7E-05	7E-04

Key: WD = wood density (gcm^{-3}), C =carbon (%), N = Nitrogen, Cg =carbon (gcm^{-3}), Ng = Nitrogen (gcm^{-3})

Although the spectra has some information, prediction performance was insufficient to be above the recommended Infrared Spectroscopy to be a practical method for direct determination of wood density and carbon content across species when different percentages were used.

4.11.6 *Eucalyptus camaldulensis* **as a calibration set (n=116)**

The genus *Eucalyptus* has over 800 species; among which *E. camaldulensis*, *E. saligna* and *E. grandis* are some of the most important commercial timber species which are exotic and widely planted in Yala basin. *E. camaldulensis* had the highest number of cores recorded from the field data. This was done in answering the question whether a single tree species could be used to predict the properties of other nineteen different species.

For the carbon and wood density NIR model, the calibration model performed poorly as the model developed using the MIR, with the R^2 value calibration of 0.54 and 0.56 for wood density and carbon respectively; while the other wood properties had $R^2 < 0.50$ (Table 29, Figure 30) with lowest root mean square error of validation reported for carbon (0.01). Calibration set for MIR shows slight improvement for carbon with $R^2 = 0.61$ low standard error of prediction of 0.01 was found for MIR (Figure 29).
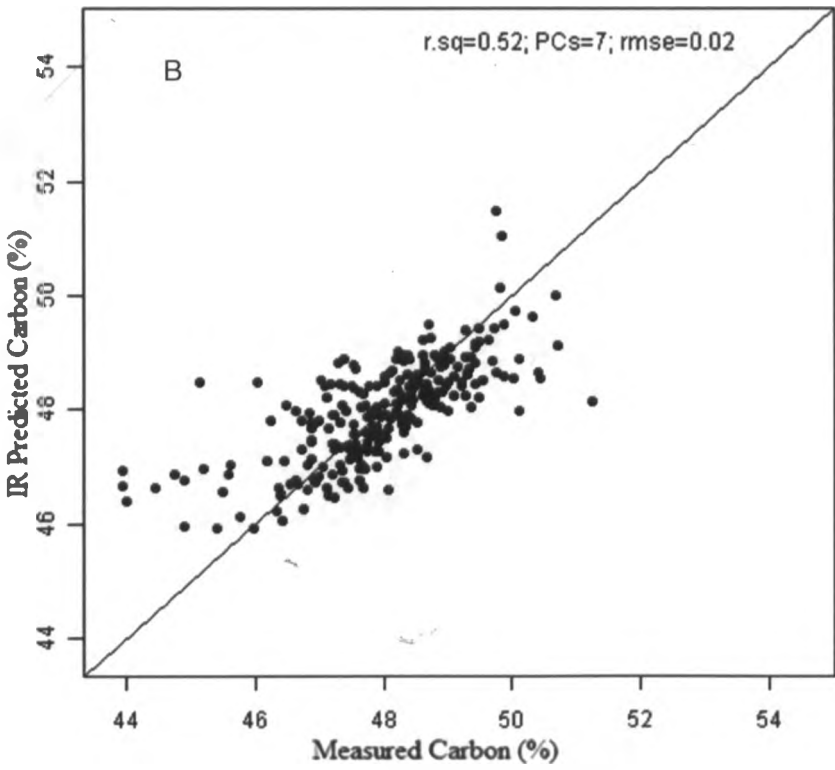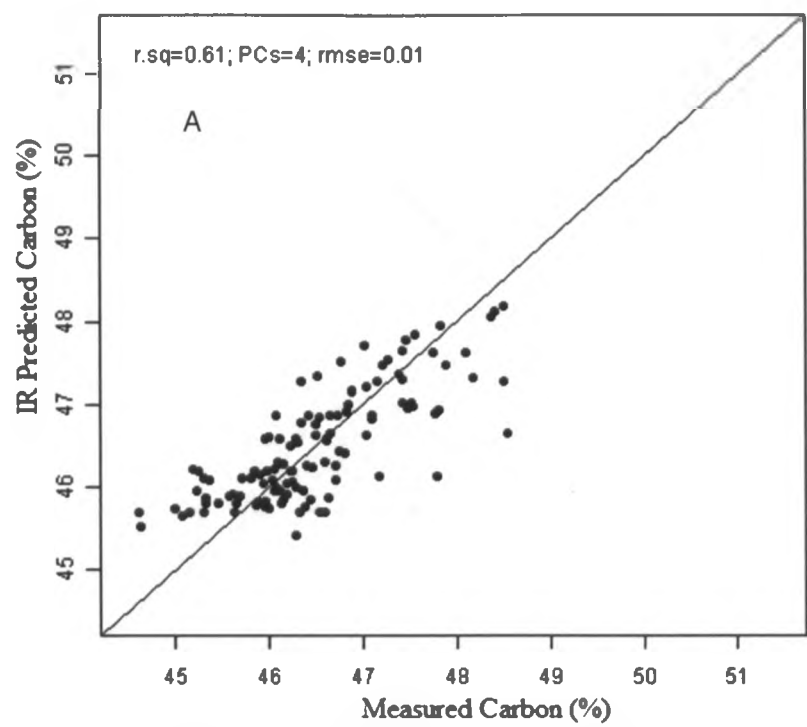
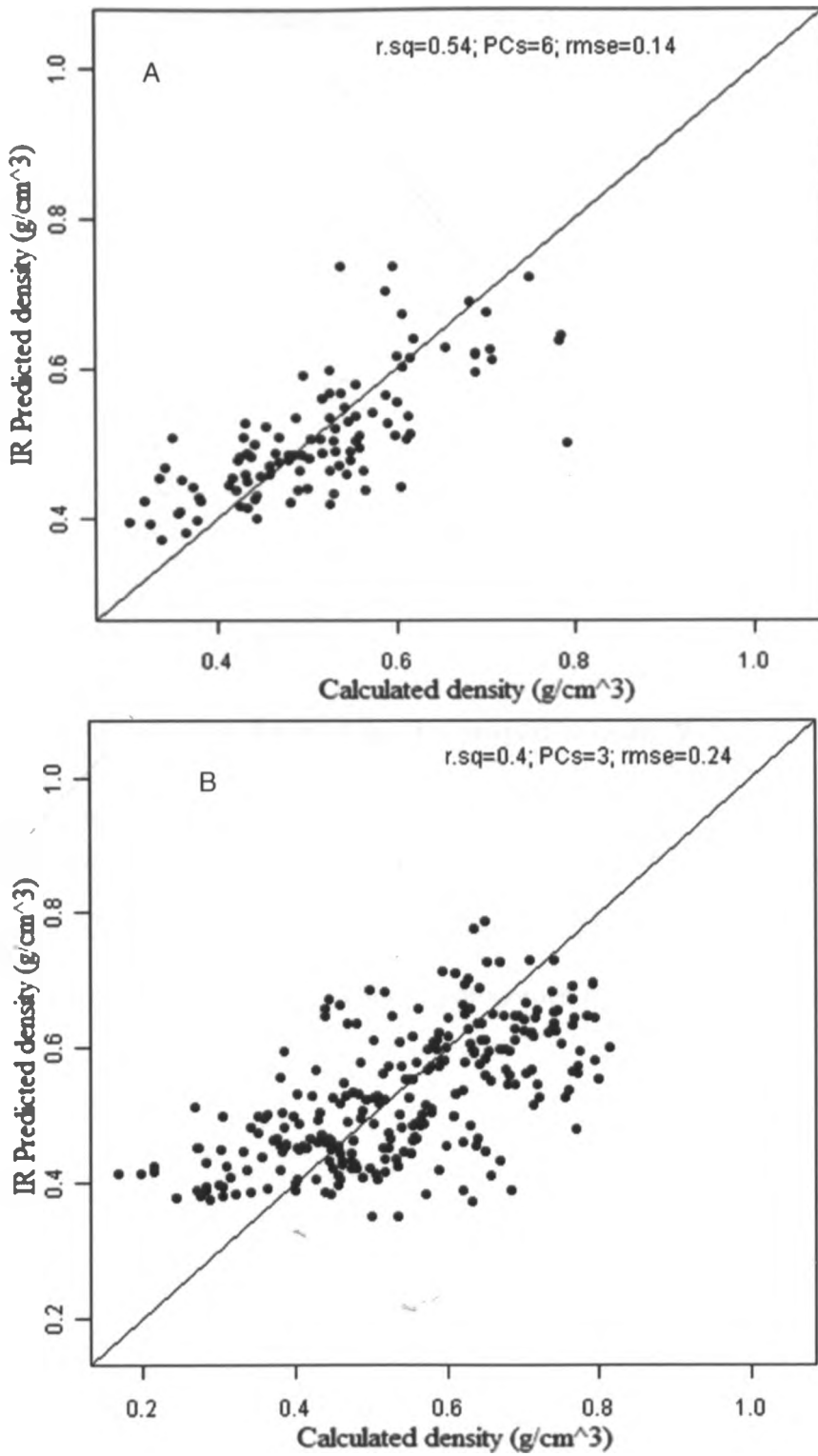Figure 29: MIR PLS models for carbon (A) Calibration and (B) validation.

Figure 30: NIR PLS models for density (A) Calibration and (B) validation

Table 29: Cross-validated calibration and Independent validation results for NIR and
MIR region of spectra based on *E. camaldulensis*.

Calibration					Validation			
IR range	Property	R^2	RMSECV	PCs	Property	R^2	Bias	RMSEP
NIR	WD	0.54	0.14	6	WD	0.29	-0.02	0.18
	C	0.56	0.01	3	C	0.21	-4.05	12.48
	N	0.03	0.19	1	N	1E-04	-0.04	0.09
	Cg	0.55	0.19	6	Cg	0.00	0.03	0.11
	Ng	0.19	0.28	2	Ng	0.35	5E-05	6E-04
MIR	WD	0.54	0.15	3	WD	0.48	-0.03	0.18
	C	0.61	0.01	4	C	0.17	-3.93	12.80
	N	0.2	0.18	3	N	4E-05	-0.04	0.09
	Cg	0.57	0.18	3	Cg	0.002	0.04	0.11
	Ng	0.37	0.25	3	Ng	0.38	3E-05	6E-04

Key: WD = wood density (gcm^{-3}), C =carbon (%), N = Nitrogen, Cg =carbon (gcm^{-3}),
n=total number of samples

4.11.7 Prediction of mixed Species properties using *E. camaldulensis* model

Statistical summary of predictions developed using *E. camaldulensis* model is shown in
table 29. The models were poor with R^2<0.50 both for NIR and MIR, making it
impossible to predict mixed species properties using cores from only one species (Figure
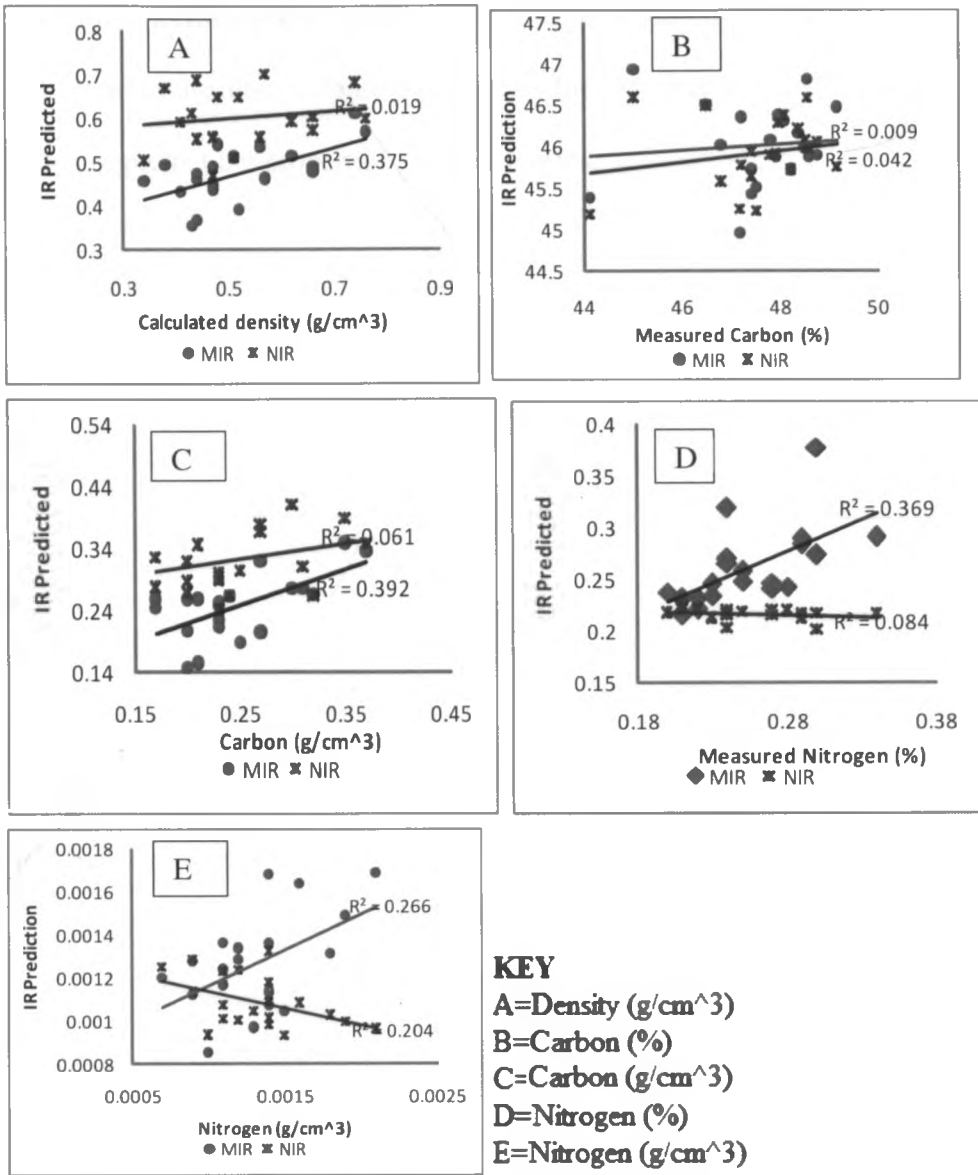31).

Figure 31: A model (*E. camaldulensis)* of IR predictions and measured values.

Nonetheless, as a result of overlapping bands, interpretation of IR spectra directly cannot be useful; the reflectance spectroscopy is based on the use of calibrations, coupled with chemometrics techniques, which utilize absorbance at many wavelengths to predict particular properties of a sample, these chemical and mechanical properties are correlated with the spectra using projection to latent structures (PLS) models.

Since the species exhibit extreme variation in wood chemistry, anatomy and physical properties the results in figure 31 supports the fact that *E. camaldulensis* species alone could not predict the properties of other species.

CHAPTER FIVE

CONCLUSIONS AND RECOMMENDATIONS

5.1 Conclusions

1. The protocol developed in this study using auger method when used correctly, appears to accurately measure wood density, carbon and nitrogen of tree species. The auger method is rapid and the field sample collection time is about 10 minutes per sample and it is capable of extracting samples from hard hardwoods. Coupled with Infrared spectroscopy, the protocol is simple to use, faster, portable and easy to handle in the field hence it can be used to acquire wood density, carbon and nitrogen data for unknown species without cutting down the trees.

2. This study provides evidence that IR techniques coupled with multivariate statistical techniques can be used to predict both physical and chemical properties of wood and it may be possible to predict properties of unknown species. This is important for field measurements where there are diverse species; however, satisfactory results were for large data sets. The result from the study shows that even though the spectra have some information, prediction performance was insufficient even with different calibration and validation percentages.

3. In developing a predictive model for wood density, carbon and nitrogen concentration for selected tree species in Yala landscapes, a strong positive relationship ($R^2=0.99$) between wood density and carbon content and also between wood density and nitrogen ($R^2=0.78$) was observed. But there was no

clear distinction observed between carbon content stored in indigenous versus exotic species. The generic 50% carbon was found to be higher compared to 47.56% reported in this study. This difference of about 2% could result in bias in carbon stock estimation. Thomas and Malczewski (2007) reported a carbon difference of 2–3% among conifers from the generic value and noted a bias of 4–6% in carbon stock assessments. Carbon content variation among species reflects differences in chemical make up's and because wood density is easier and cheaper to measure than C concentration, developing calibrations with only one species was not possible.

4. While predicting physical and chemical properties of tree species using NIR/MIR spectral regions, NIR predictive model gave better predictions for all the properties ($R^2 > 0.80$) except for wood density estimation where MIR performed better with $R^2 = 0.81$. A prediction performance with R^2 values of 0.75 and above are considered good (Kelly *et al.,* 2004) for heterogeneous material such as wood.

5. Finally, the study further demonstrated that Fourier transform Spectroscopy in the infrared domain continues to be an attractive technique in predicting physical and chemical characteristic of tree species due to its fast analysis time (seconds), moderate cost, shorter sample preparation time and reproducible results.

5.2 Recommendations

1. Applications of Fourier transform Infrared Spectroscopy is a robust approach to tree physical and chemical properties analysis.

2. This research work was limited to few tree species suggesting further work on improving the prediction accuracy by increasing sample size and incorporating more diverse species to draw meaningful inferences about predicting properties.

3. The observed strong relationship between wood density and carbon-nitrogen content should be explored to develop a carbon-nitrogen database. The database will be useful for C stock estimation and supplement the existing wood density databases for species specific values in biomass estimation.

4. The estimation of carbon-nitrogen in trees gave an illustrative assessment of carbon-nitrogen storage within the habitats sampled. Other carbon pools are likely to follow a similar pattern with agricultural intensification.

5. Pre-processing transformations of spectral data constituted an important step in multivariate calibration and improved the accuracy of prediction models. However, other methods of spectral pre-processing techniques need to be tried when dealing with diverse set of tree species.

REFERENCES

Abdi, H. (2003) PLS-regression: Multivariate analysis. In: M. Lewis-Beck, A. Bryman and T. Futing, Editors, Encyclopaedia for Research Methods for the Social Sciences, Sage, Thousand Oaks, CA.

Acuna, M.A. and Murphy, G.E. (2006) Use of near Infrared Spectroscopy and multivariate analysis to predict wood density of Douglas-fir from chain saw chips. Forest Products Journal 56 (12):67-72.

ASTM Annual Book of Standards. (1998) Standard Practices for Infrared, multivariate, quantitative analysis (E 1655-97), 3(06), West Conshohocken.

Ayala, F.J. and Kiger, J.A. (1984) Modern Genetics. Benjamin/Cummings press, Menlo Park, London

Baker,T. R., Phillips, O. L., Malhi, Y., Almeida, S., Arroyo, L., Difiore, A., Erwin, T., Killeen, T. J., Laurance, S. G., Laurance, W. F., Lewis, S. L., Lloyd, J., Monteagudo, A., Neill, D.A., Patino, S., Pitman, N.C.A., Silva, J.N.M. and Vasquez Martinez, R. (2004) Variation in wood density determines spatial patterns in Amazonian forest biomass. Global Change Biology 10:545–562.

Banwell, C.N. (1983) Fundamentals of Molecular Spectroscopy, (3rd Edn) McGraw-Hill, London.

Batten, G.D., Blakeney, A.B., (1992) In: Hildrum, K.I., Isaksson, T., Naes, T., and Berg, A., (eds) Near infra-red Spectroscopy—bridging the gap between data analysis and NIR applications. Ellis Horwood, Chichester, pp 185–190.

Bellon-Maurel, V., and McBratney, A. (2011) Near-Infrared (NIR) and mid-Infrared (MIR) spectroscopic techniques for assessing the amount of carbon stock in soils- Critical review and research perspectives, Soil Biology and Biochemistry.

Blanco, M., and Villarroya, I. (2002) NIR Spectroscopy: a rapid-response analytical tool. Trends in Analytical Chemistry, 21(4):240–250.

Boye, A., Verchot, L., and Zomer, R. (2008) Baseline Report–Yala and Nzoia River Basins: Western Kenya Integrated Ecosystem Management Project Findings from the baseline surveys, World Agroforestry Centre, Nairobi.

Brown, S. (2002) Measuring carbon in forests: Current status and future challenges. Environmental Pollution 116:363–372.

Carsan, S., Stroebel, A., Harwood, C., Kindt, R., Kinga, P., Orwa, C., Nzisa, A., Neufeldt, H. and Jamnadass, R. (2012) The African wood density database. The World Agroforestry Centre, Nairobi.

Chalmers, J. M. and Griffiths, P. R. (eds) (2002) Handbook of Vibrational Spectroscopy, Volume 1: Theory and Instrumentation. John Wiley and Sons, Ltd, ISBN-13: 978-0471988472.

Chang, C.W. and Laird, D.A. (2002) Near-Infrared reflectance Spectroscopy analysis of soil C and N. Soil Science, 167(2):110-116.

Chave, J., Andalo, C., Brown, S., Cairns, M. A., Chambers, J.Q. and Eamus, D. (2005) Tree allometry and improved estimation of carbon stocks and balance in tropical forests. Oecologia, 145, 87-99.

Chave, J., Coomes, D., Jansen, S., Lewis, S.L., Swenson, N.G., and Zanne, A.E. (2009) Towards a worldwide wood economics spectrum. Ecology Letters 12:351–366.

Chodak, M., Maria N., and Friedrich B. (2007) Near-Infrared Spectroscopy for analysis of chemical and microbiological properties of forest soil organic horizons in a heavy-metal-polluted area. Biology and Fertility of *Soils* 44(1):171-180.

Christophe, P., and Grégoire, L. A. (2001) Wood formation in trees. Plant Physiology 127:1513-1523.

Costa e Silva, J., Borralho, N.M.G., Araújo, J.A., Vaillancourt, R.E. and Potts, B.M. (2009) Genetic parameters for growth, wood density and pulp yield in Eucalyptus globulus. Tree Genet Genom 5:291–305.

Cown, D.J., Young, G.D and Burdon, R.D. (1992) Variation in wood characteristics of 20 year old half - sib families of Pinus radiata. New Zealand Journal of Forestry Science 22(1): 63-76.

Cozzolino, D., and Moron, A. (2006) Potential of near-Infrared reflectance Spectroscopy and chemometrics to predict soil organic carbon fractions. Soil and Tillage Research 85: 78–85.

Cozzolino, D., Holdstock, M., Dambergs, R.G., Cynkar, W.U. and Smith, P.A. (2009) Mid Infrared Spectroscopy and multivariate analysis: A tool to discriminate between organic and non-organic wines grown in Australia. Food Chemistry, 116 (3):761-765.

De Castro, F., Williamson, G.B. and de Jesus, R.M. (1993) Radial variation in wood specific gravity of *Joannesia princeps*: the roles of age and diameter. Biotropica, 25(2): 176-182.

Defo, M., Taylor, A. M., and Bond, B. (2007) Determination of moisture content and density of fresh-sawn red oak lumber by near Infrared Spectroscopy, Forest Prod. J. 57(5):68-72.

Desch, H.E. and Dinwoodie, J.M. (1996) Timber: structure, properties, conversion and use. 7th edition. MacMillan Press Ltd., London. p.306.

Dewar, R.C. (1990) A model of carbon storage in forests and forest products. Tree Physiology 6:417-428.

Elias, M. and Potvin, C. (2003) Assessing inter and intra-specific variation in trunk carbon concentration. Canadian Journal of forestry Research 33:1039–1045.

Flores, O. and Coomes, D. A. (2011) Estimating the wood density of species for carbon stock assessments. Methods in Ecology and Evolution, 2: 214–220.

Francis, J.K. (1994) Simple and inexpensive method for extracting wood density samples from tropical hardwoods. Tree Plant. Not. 45(1):10–12.

Gindl, W., Teischinger, A., Schwanninger, M. and Hinterstoisser, B. (2001) The relationship between near Infrared spectra of radial wood surfaces and wood mechanical properties, Journal of Near Infrared Spectroscopy.9:255-261.

Givens, D.I., and Deaville, E.R. (1999) The current and future role of near Infrared reflectance Spectroscopy in animal nutrition: a review. Aust. J. Agric. Res.50:1131-1145.

Glenday, J. (2006) Carbon storage and emissions offset potential in an East African tropical rainforest. Forest Ecology Management, 235, 72-83.

Gribbin, J., (1990) Hothouse Earth, the Greenhouse Effect and Gaia, London.

Hacke, U. G., Sperry, J S., Pockman, W. T., Davis, S. D. and Mcculloh, K. A. (2001) Trends in wood density and structure are linked to prevention of xylem implosion by negative pressure. Oecologia 126:457–461.

Hein, P. R. G., Lima, J. T., and Chaix, G. (2009) Robustness of models based on near Infrared spectra to predict the basic density in *Eucalyptus urophylla* wood. Journal of Near Infrared Spectroscopy 17(3):141–150.

Henry, M., Besnard, A., Asante, W., Eshun, J., Adu-Bredu, S., Valentini, R., Bernoux, M. and Saint-André, L. (2010) Wood density, phytomass variations within and among trees, and allometric equations in a tropical rainforest of Africa. Forest Ecology and Management 260(8): 1375-1388.

Hillis, W.E. (1978) Wood quality and utilization. In: Eucalypts for Wood Production Hillis, W.E. and Brown, A.G. (eds). CSIRO, Melbourne, Australia, pp. 259–289.

Hoffmeyer, P. and Pedersen, J.G. (1995) Evaluation of density and strength of Norway spruce wood by near Infrared reflectance Spectroscopy. Holz als Roll- und Werkstoff 53:165-170.

Houghton, R.A., (1996) Converting terrestrial ecosystems from sources to sinks of carbon. AMBIO 267–272.

Ichami, S.M (2008) Diagnosis of Soil and Plant Nutrient Constraints in Small-scale Groundnut Production Systems using Infared Spectroscopy in Western Kenya. Department of Land Resource Management and Agricultural Technology. Msc thesis, University of Nairobi.

Iida, Y., Poorter, L., Sterck, F.J., Kassim, A.R., Kubo, T. and Potts, M.D. (2011) Wood density explains architectural differentiation across 145 co-occurring tropical tree species. Functional Ecology, 26, 274-282.

Ilic, J., Boland, D., Mcdonald, M., Downes, G. and Blakemore, P. (2000) Wood Density Phase1-State of Knowledge, National Carbon Accounting System. Australian Greenhouse Office, Commonwealth of Australia. Technical Report, No. 18, pp 218.

Janik, L. J., Merry, R. H., and Skjemstad, J. O. (1998) Can mid-Infrared diffuse reflectance analysis replace soil extractions? Australian Journal of Experimental Agriculture 38:681–696.

Jones, P.D., Schimleck, L.R., Peter, G.F., Daniels, R.F., and Clark III, A. (2006) Non-destructive estimation of wood chemical composition of sections of radial strips by diffuse reflectance near Infrared Spectroscopy. Wood Science and Technology 40:709-720.

Jozsa, L.A. and Middleton, G.R. (1994) A discussion of wood quality attributes and their practical implications. Forintek Canada Corp., Vancouver, B C. Special Publ. No. SP-34.

Juday, G. P. (2010) Climate change in relation to carbon uptake and carbon storage in the Arctic. International Arctic Science Committee. Section 14.10 of the Arctic Climate Impact Assessment.

Kelley, S.S., Rials, T.G., Snell, R., Groom, L.H. and Sluiter, A. (2004) Use of near Infrared Spectroscopy to measure the chemical and mechanical properties of solid wood. Wood Science Technology 38:257-276.

Kirby, K.R, and Potvin. C. (2007) Variation in carbon storage among tree species: implications for the management of a small scale carbon sink project. Forest Ecology Management 246:208–221.

Koch, L. and Fins, L. (2000) Genetic variation in wood specific gravity from progeny tests of ponderosa pine (*Pinus ponderosa* L.) in northern Idaho and western Montana. Silvae Genetica, 49, 174-181.

Kooistra, L., Wanders, J., Epema, G.F., Leuven, R.S., Wehrens, R., and Buydens, L.M.C. (2003) The potential of field Spectroscopy for the assessment of sediment properties in river floodplains. Analitica Chimica Acta 484:189–200.

Kozlowski, T.T. (1992) Carbohydrate sources and sinks in woody-plants, Bot. Rev.58:107–222.

Lamlom, S.H., and Savidge, R.A. (2003) A reassessment of carbon content in wood: variation within and between 41 North American species. Biomass and Bioenergy 25: 381–388.

Lindzen, R.S. (1997) Can increasing atmospheric CO2 affect global climate? Proc. Natl..Acad. Sci. USA, 94:8335-8342.

Ludwig, B., Khanna, P. K., Bauhus, J., Hopmans, P. (2002) Near Infrared Spectroscopy of forest soils to determine chemical and biological properties related to soil sustainability. Forest Ecology and Management 171:121–132.

Ludwig, B., Nitschke, R., Michel, K., Terhoeven-Urselmans, T., and Flessa, H. (2008) Use of mid-Infrared Spectroscopy for the prediction of the composition of organic matter in soil and litter. Journal of Plant Nutrition and Soil Science 171: 384–391.

Madari, B.E., Reeves, J.B., Coelho, M.R., Machado, P.L.O.A., De-Polli, H., Coelho, R.M., Benites, V.M., Souza, L.F. and McCarty, G.W. (2005) Mid- and near-Infrared spectroscopic determination of carbon in a diverse set of soils from the Brazilian National Soil Collection. Spectroscopy Letters 38(6):721–740.

Magnani, F., Mencuccini, M., Borghetti, M., Berbigier, P., Berninger, F., Delzon, S., Grelle, A., Hari, P., Jarvis, P.G., and Kolari, P. (2007) The human footprint in the carbon cycle of temperate and boreal forests. Nature 447:849–851.

Martens, H. and Naes, T. (1991) Multivariate Calibration. Wiley, Chichester, 438 pp.

McCarty, G.W., Reeves III, J.B., Reeves, V.B., Follett, R.F., and Kimble, J.M. (2002) Mid-Infrared and near-Infrared diffuse reflectance Spectroscopy for soil carbon measurement. Soil Sci. Soc. Am. J. 66: 640–646.

Melillo, J.M., Aber, J.D and Muratore, J.F. (1982) Nitrogen and Lignin Control of Hardwood Leaf Litter Decomposition Dynamics. Ecological Society of America. Ecology 63(3):621-626.

Michel, K., Bruns, C., Terhoeven-Urselmans, T., Kleikamp, B. and Ludwig, B. (2006) Determination of chemical and biological properties of composts using near Infrared Spectroscopy. J. Near Infrared Spectrosc. 14:251–259.

Mroczyk, W.B., Kasprzyk, H. and Gawecki, T. (1992) In Making Light Work: Advances in Near Infrared Spectroscopy, Ed by Murray, I. and Cowe, I.A. Verlagsgesellschaft, Weinheim, p. 566.

Muller-Landau, H. C. (2004) Interspecific and inter-site variation in wood specific gravity of tropical trees. Biotropica. 36: 20 – 32.

Naes, T., Isaksson, T., Fearn, T. and Davies, T. A. (2002) User Friendly Guide to Multivariate Calibration and Classification; NIR Publications: Chichester, West Sussex, UK.

Nock, C.A., Geihofer, D., Grabner, M., Baker, P.J., Bunyavejchewin, S. and Hietz, P. (2009) Wood density and its radial variation in six canopy tree species differing in shade-tolerance in western Thailand. Annals of botany 104: 297-306.

Nogueira, E.M., Fearnside, P.M. and Nelson, B.W. (2008) Normalization of wood density in biomass estimates of Amazon forests. Forest Ecology and Management 256: 990–996.

Norby, R.J., Warren, J.M., Iversen, C.M., Medlyn, B.E. and McMurtrie, R.E. (2010) CO2 enhancement of forest productivity constrained by limited nitrogen availability. Proceedings of the National Academy of Sciences USA 107(19):368-373

O'sullivan, P. (1976) The influence of initial espacement and thinning regime upon wood density in Sitka spruce (*Picea sitchensis*). M.Agr.Sc. Thesis, University College Dublin.

Osborne, B.G., Fearn, T. and Hindle, P.H. (1993) Practical NIR Spectroscopy with applications in food and beverage analysis. Second Edition. Longman Scientific and Technical, Harlow, Essex, UK. pp. 227.

Payne, R.W., Murray, D.A., Harding, S.A., Baird, D.B. and Soutar, D.M. (2009) GenStat for Windows (12th Edition) Introduction.VSN International, Hemel Hempstead.

Pedersen, J.G., Hoffmeyer, P., Jacobsen, U.G. and Reffstrup, T. (1993) Non-Destructive Evaluation of Wood by Near Infrared Reflectance Spectroscopy. Report no. 93-1-1, Biotechnological Institute, Kolding, Denmark.

Petisco, C., García-Criado, B., Vázquez de Aldana, B .R., Zabalgogeazcoa, I., Mediavilla, S., and García-Ciudad. (2005) Use of near-Infrared reflectance Spectroscopy

in predicting nitrogen, phosphorus and calcium contents in heterogeneous woody plant species. Analytical and bioanalytical chemistry 382(2):458-65.

Pettersen, R.C. (1984) The Chemical Composition of Wood. In The Chemistry of Solid Wood, by Roger Rowell, 57-126. American Chemical Society.

Pliura, A., Zhang, S.Y., Mackay, J. and Bouequet, J. (2007) Genotypic variation in wood density and growth traits of poplar hybrids at four clonal trials. Forest Ecology and Management 238: 92–106.

Preston, C.M. and Schmidt, M.W.I. (2006) Black (pyrogenic) carbon: a synthesis of189 current knowledge and uncertainties with special considerations of boreal regions. 190 Biogeosciences 3: 397-420.

Quanzhi, C., Wang, Xingchang, W. and Xiankui, Q. (2009) Carbon concentration variability of 10 Chinese temperate tree species. Forest Ecology and Management 258:722–727

R Development Core Team (2005) R: A language and environment for statistical computing, reference index version 2.12.1. R Foundation for Statistical Computing, Vienna, Austria. ISBN 3-900051-07-0, URL http://www.R-project.org.

Reeves III, J.B., (1994) Near-versus mid-Infrared diffuse reflectance Spectroscopy for the quantitative determination of the composition of forages and by-products. J. Near Infrared Spectrosc. 2: 49–57.

Reyes, G., Brown, S., Chapman, J. and Lugo, A.E. (1992) Wood densities of Tropical tree species. http://www.srs.fs.usda.gov/pubs/gtr/gtr_so088.pdf [accessed on 2nd November 2011].

Rossel, V., McGlynn, A. and McBratney, A. B. (2006) Determining the composition of mineral-organic mixes using UV-Vis–NIR diffuse reflectance Spectroscopy. Geoderma 137: 70–82.

Rueda, R., Williamson, G.B. (1992) Radial and vertical wood specific gravity in *Ochroma pyramidale* (Cay. ex Lam.) Urb. (Bombacaceae), Biotropica, 24:512-518.

Schimleck, L.R. and French, J. (2001) Application of NIR Spectroscopy to clonal *Eucalyptus globulus* samples covering a narrow range of pulp yield. Appita 55(2):149-154.

Schimleck, L.R., Evans, R. and Ilic, J. (2001) Estimation of *Eucalyptus delegatensis* wood properties by near Infrared Spectroscopy. Can. J. For. Res., 31: 1671-1675.

Schimleck, L.R., Michell, A.J., Raymond, C.A. and Muneri, A. (1999) Estimation of basic density of *Eucalyptus globulus* using near-Infrared Spectroscopy. Can. J. For. Res., 29: 194-201.

Schlesinger, W.H. (1991) Biogeochemistry: An Analysis of Global Change. Academic Press, San Diego.

Shepherd, K.D. and Walsh, M.G. (2002) Development of reflectance spectral libraries for characterization of soil properties. Soil Science Society of America Journal, 66(3): 988-998.

Shepherd, K.D. and Walsh, M.G. (2007) Infrared Spectroscopy-enabling an-evidence based diagnostic surveillance approach to agricultural and environmental management in developing countries. Journal of near Infrared Spectroscopy 15: 1-19.

Sherman, C.P. (1997) Infrared Spectroscopy in Handbook of Instrumental Techniques for Analytical Chemistry, edited by Settle F, Prentice Hall PTR, New Jersey, USA, pp.247-282.

Skaar, C. (1972) Water in Wood, Syracuse University Press, Syracuse, NY, 218 pp.

Small, Gary W. (2006) Chemometrics and near-Infrared Spectroscopy: Avoiding the pitfalls. Trends in Analytical Chemistry 25(11): 1057-1066.

So, C.L., Lebow, S.T., Groom, L.H. and Rials, T.G. (2004) The application of near Infrared (NIR) Spectroscopy to inorganic preservative treated wood. Wood and Fiber Science. 36(3):329-336.

Stark, E.W. (1988) Calibration methods for NIR analysis. In: Creaser, C.S., Davies, A.M.C. (Eds.), Analytical applications of Spectroscopy, Royal Society of Chemistry, London, United Kingdom, pp. 21–34.

Suddick, E.C., Whitney, P., Townsend, A.R and Davidson, E. A. (2012) The role of nitrogen in climate change and the impacts of nitrogen–climate interactions in the United States: foreword to thematic issue. Biogeochemistry 110:1-3

Swierenga, H. (2000) Robust multivariate calibration models in vibrational spectroscopic applications, PhD Thesis. Catholic University of Nijmegen, Netherlands.

Thomas and Malczewskia (2007) Wood carbon content of tree species in Eastern China: Interspecific variability and the importance of the volatile fraction. Journal of Environmental Management 85:659–662.

Thomas, S.C., (1996) Asymptotic height as a predictor of growth and allometric characteristics in Malaysian rain forest trees. American Journal of Botany 83:556–566.

105

Thompson, D.A., and Matthews, R.W. (1989) The Storage of Carbon in Trees and Timber, Forestry Commission Research Information Note 160. Transworld Publishers Ltd.

Thygesen, L.G. (1994) Determination of dry matter content and basic density of Norway spruce by near Infrared reflectance Spectroscopy. Journal of near-Infrared Spectroscopy 2:127-135.

Treacy, M., Evertsen, J. and Dhubháin, Á.N. (2000) A comparison of mechanical and physical wood properties of a range of Sitka spruce provenances. National council of forest research and development (COFORD).University College Dublin.

UNEP. (2009) Carbon Benefits Project (CBP): Modelling, Measurement and Monitoring (PG 41).

Vasques, G.M., Grunwald, S. and Sickman, J.O. (2008) Comparison of multivariate methods for inferential modelling of soil carbon using visible/near-Infrared spectra. Geoderma 146:14–25.

Viscarra, R.A., Walvoort, D.J., McBrateny., A, Janik, L.J. and Skjemstad, J.O. (2006) Visible near Infrared, mid Infrared or combined diffuse reflectance Spectroscopy for simultaneous assessment of various soil properties. Geoderma 131:59–75.

Williamson, G.B., and Wiemann, M.C. (2010) Measuring wood specific gravity...Correctly. American Journal of Botany 97(3): 519-524.

Wu, Shi-jun, Jian-min Xu, G-you Li, VuokkoRisto, Zhao-hua Lu, B-qi Li. and Wei Wang. (2010) Use of the Pilodyn for assessing wood properties in standing trees of Eucalyptus clones. Journal of Forestry Research 21(1): 68-72.
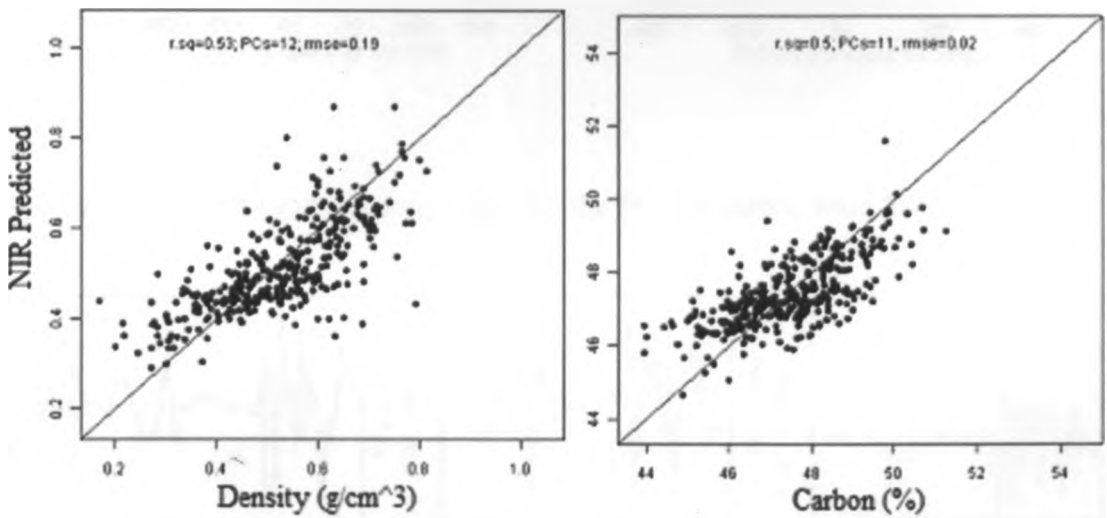
Zobel, B.J. and Van Buijtenen, J.P. (1989) Wood variation: its causes and control. Berlin, Springer-Verlag 418p.
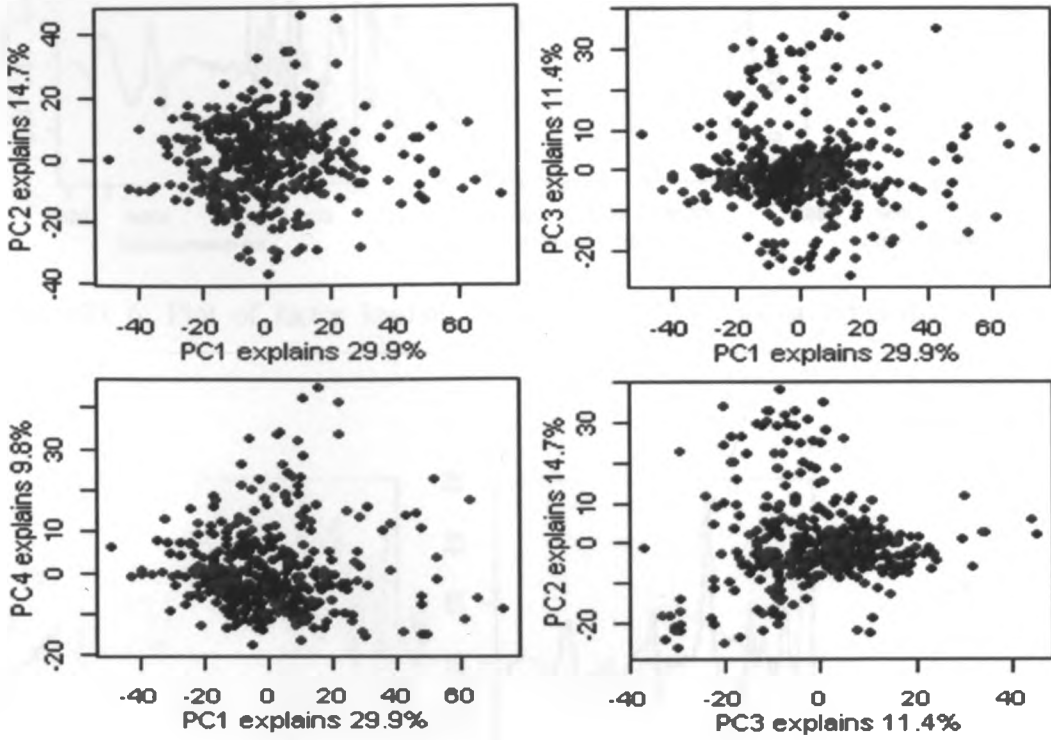
APPENDICES

Appendix 1: NIR PLS Calibration models for nitrogen and Carbon (all samples set).
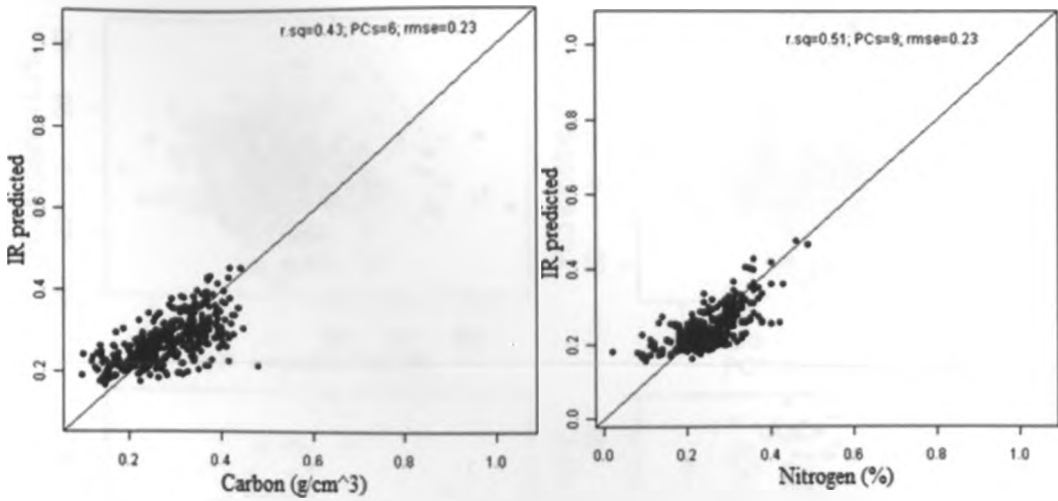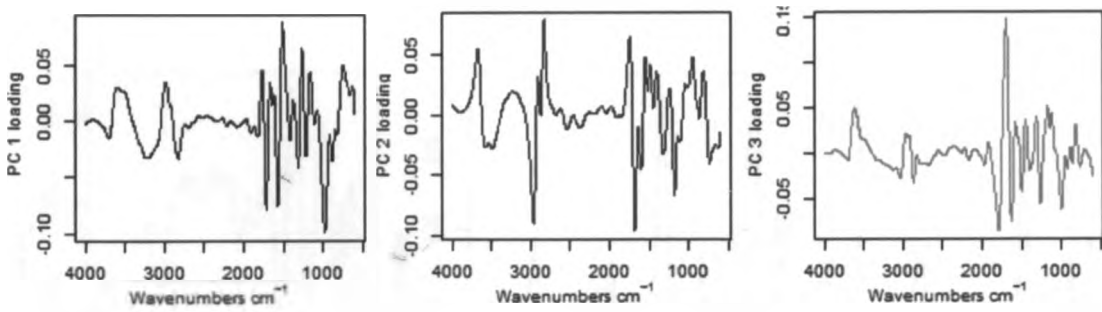

Appendix 2: NIR PLS Calibration models for nitrogen and Carbon and nitrogen (90% Calibration set).

Appendix 3: Samples selection based on spectral diversity. Red dots indicates selected calibration samples set.
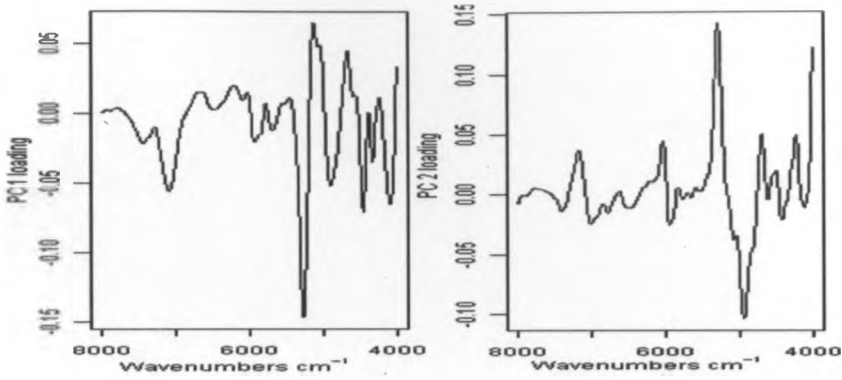

Appendix 4: Plot of factor loading values for the PCs for carbon from MIR spectra.

Appendix 5: Plot of factor loading values for the PCs for nitrogen from MIR spectra.
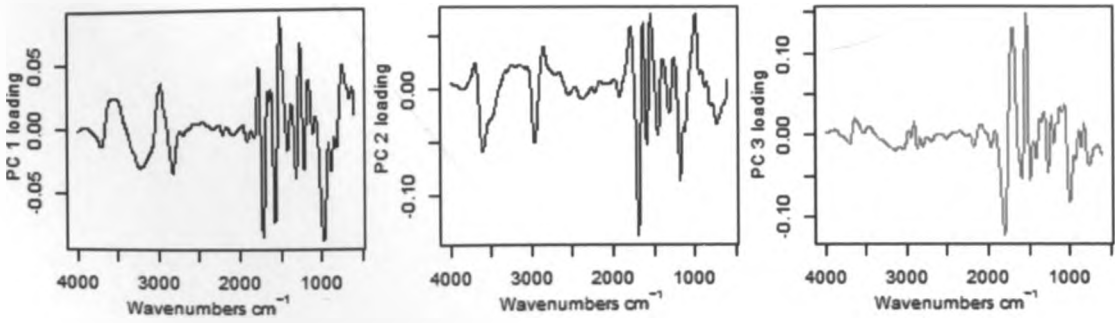
Appendix 6: Plot of factor loading values for the PCs for wood density from NIR spectra.

Appendix 7: Plot of factor loading values for the PCs for carbon from NIR spectra.